NIH Public Access
Author Manuscript
Dev Biol. Author manuscript; available in PMC 2013 December 02.

Published in final edited form as:
Dev Biol. 2008 January 15; 313(2): . doi:10.1016/j.ydbio.2007.11.014.

The *Caenorhabditis elegans* NR4A nuclear receptor is required for spermatheca morphogenesis

Chris R. Gissendanner[1,*], **Kristopher Kelley**[1], **Tri Q. Nguyen**[2,#], **Marius C. Hoener**[2,#], **Ann E. Sluder**[3,%], and **Claude V. Maina**[4]

[1]Department of Biology, University of Louisiana at Monroe, LA 71209, USA [2]F. Hoffmann-La Roche, Basel, Switzerland [3]Cambria Biosciences LLC, Woburn MA 01801, USA [4]New England Biolabs, Ipswich, MA, 01938-2723, USA

Abstract

The gene *nhr-6* encodes the *Caenorhabditis elegans* ortholog of the NR4A nuclear receptor. We determined the biological functions of NHR-6 through the isolation and characterization of a deletion allele of *nhr-6, lg6001*. We demonstrate that *nhr-6* has an essential role in the development of the *C. elegans* somatic gonad. Specifically, *nhr-6* is required for the development of the hermaphrodite spermatheca, a somatic gonad organ that serves as the site of sperm storage and oocyte fertilization. Using a variety of spermatheca cell markers, we have determined that loss of *nhr-6* function causes severe morphological defects in the spermatheca and associated spermathecal valves. This appears to be due to specific requirements for *nhr-6* in regulating cell proliferation and cell differentiation during development of these structures. The improper development of these structures in *nhr-6(lg6001)* mutants leads to defects in ovulation and significantly reduced fecundity of *C. elegans* hermaphrodites. The phenotypes of *nhr-6(lg6001)* mutants are consistent with a role for *nhr-6* in organogenesis, similar to the functions of its mammalian homologs.

Keywords

nhr-6; NR4A; *C. elegans*; spermatheca; spermatheca-uterine valve

INTRODUCTION

The formation of organs requires the precise regulation and coordination of cell proliferation, differentiation, morphogenesis and growth (Sears and Nevins, 2002; Vidwans and Su, 2001). The nematode *Caenorhabditis elegans* is an outstanding model for the genetic dissection of organ formation. The invariant cell lineage allows for the analysis of organ formation to be performed at the single-cell level which, in turn, provides a framework for

© 2007 Elsevier Inc. All rights reserved.

[*]Corresponding author: gissendanner@ulm.edu, 318-342-3314, FAX 318-342-3312 .
[#]Work performed at EleGene AG, formerly of Martinsreid, Germany. Current address is F. Hoffmann-La Roche.
[%]Current address: Scynexis, Research Triangle Park, NC, 27709, USA

Publisher's Disclaimer: This is a PDF file of an unedited manuscript that has been accepted for publication. As a service to our customers we are providing this early version of the manuscript. The manuscript will undergo copyediting, typesetting, and review of the resulting proof before it is published in its final citable form. Please note that during the production process errors may be discovered which could affect the content, and all legal disclaimers that apply to the journal pertain.

NIH-PA Author Manuscript
NIH-PA Author Manuscript
NIH-PA Author Manuscript

NIH-PA Author Manuscript

NIH-PA Author Manuscript

NIH-PA Author Manuscript

the careful dissection of genetic processes regulating proliferation and differentiation of various organ lineages (Kipreos, 2005).

An adult *C. elegans* hermaphrodite consists of only 959 somatic cells (Kimble and Hirsh, 1979; Sulston and Horvitz, 1977). Nonetheless, *C. elegans* possesses several complex organ systems. For example, the egg-laying machinery of *C. elegans* requires the coordinated development of two organs, the vulva and uterus. The genes that have been identified in the genetic analysis of these organ systems have provided insight into the cell-cell signaling processes that regulate cell division patterns, cell differentiation, morphogenesis, and the development of the physical interactions between these two interconnected organs (Newman et al., 1999; Newman et al., 2000; Palmer et al., 2002; Rajakumar and Chamberlin, 2006; Wang and Sternberg, 2001).

Despite this progress, much remains to be understood about the organ formation process. One area of interest is the role of transcription factors in coordinating lineage-specific patterns of cell division and differentiation. Transcription factors that function during organogenesis must have the ability to respond to and integrate multiple signaling pathways to control cell proliferation and cell differentiation. One group of transcription factors that have this ability are the nuclear receptors (NRs), among the most important regulators of gene expression in the metazoa. NRs are a diverse group of transcription factors that are unique in their ability to regulate the expression of specific genes in response to a wide variety of intercellular and intracellular signals (Mangelsdorf et al., 1995). The most intensively studied and well understood NRs are those that function as receptors for signaling molecules such as endocrine hormones and cellular metabolites. In addition to the regulation of core cell physiological processes, NRs also function as key transcriptional regulators during development. Common developmental functions of NRs include early embryonic patterning, cell fate specification, organogenesis and invertebrate life cycle progression (Giguere, 1999; King-Jones and Thummel, 2005).

One particular group of NRs, NR4A, has recently emerged as developmentally important transcriptional regulators. Structural studies have demonstrated that NR4A NRs are not ligand regulated in the canonical NR fashion (Wang et al., 2003). Therefore, it is likely that NR4A NRs are true unliganded (orphan) receptors that mediate cellular processes through interactions with signal transduction pathways (Maira et al., 2003; Pekarsky et al., 2001; Swanson et al., 1999; Wang et al., 2003; Wingate et al., 2006). The three mammalian paralogs of the NR4A subgroup (NR4A1, NR4A2, and NR4A3) have been implicated in a vast array of biological processes including immune system development, metabolism, inflammation, atherogenesis, steroidogenesis, central nervous system development, and organogenesis (Maxwell and Muscat, 2006). Despite their biological importance, much remains to be learned regarding the precise functions and cellular regulation of these transcription factors. However, organogenesis, tissue differentiation, and cell proliferation in multiple contexts appear to be important biological functions of the NR4A subgroup (Castro et al., 2001; Kolluri et al., 2003; Martinez-Gonzalez et al., 2003; Suzuki et al., 2003; Zeng et al., 2006). As examples of this, Nurr1 (NR4A2) has been established to be a critical differentiation factor for mid-brain dopaminergic neurons (Zetterstrom et al., 1997) and NOR-1 (NR4A3) is required for the proliferation and differentiation of inner ear epithelia, as well as hippocampal and pyramidal cell development (Ponnio et al., 2002; Ponnio and Conneely, 2004).

Here we characterize the developmental functions of *nhr-6*, the sole NR4A homolog encoded in the *C. elegans* genome (Sluder and Maina, 2001). We present evidence that *nhr-6* is important for reproduction in *C. elegans* and is required for proper morphogenesis of the spermatheca, a component of the *C. elegans* somatic gonad involved in oocyte ovulation and

NIH-PA Author Manuscript

NIH-PA Author Manuscript

NIH-PA Author Manuscript

fertilization. We also demonstrate that *nhr-6* has specific functions in cell proliferation and cell differentiation during development of the spermatheca and spermatheca-uterine valve. This work establishes *nhr-6* as a model system for investigating the cellular activities of NR4A in the regulation of gene expression during development, and also establishes the spermatheca as an additional *C. elegans* system for investigating the genetic regulation of organogenesis.

MATERIALS AND METHODS

Nematode strains

C. elegans was cultured using standard protocols (Brenner, 1974). The following strains were utilized in this study: N2 (Bristol); XY1004 (*nhr-6(lg6001)*); GR1371 (*eri-1(mg366)*); JJ532 (pie-1(zu154) unc-25(e156)/qC1 dpy-19(e1259) glp-1(q339)); SU93 (*jcIs1*[*ajm-1::GFP + rol-6(su1006)*]); DG1576 (*tnIs5*[*lim-7::GFP + rol-6(su1006)*]); PS3662 (*syIs63*[*cog-1::GFP + unc-119(+)*]); UA2 (*baEx2*[*lis-1::GFP + rol-6(su1006)*]); HR596 (*mel-11::GFP*); HR606 (*let-502::GFP*); MT2405 (*ced-3(n717) unc-26(e205)*; DZ325 (ezIs2[fkh-6::GFP + unc-119(+)]; him-8(e1489); CB3297 (*vab-9(e1744); him-5(e1490*); NL2099 (*rrf-3(pk1426)*; PS3411 (cog-1(sy607)/mnC1 dpy-10(e128) unc-52(e444); nhr-6(tm870).

The RNAi sensitized *fkh-6::GFP* expressing strain *rrf-3(pk1426); ezIs2* was constructed by crossing *rrf-3(pk1426)* males to *vab-9(e1744); ezIs2* hermaphrodites. *vab-9* was utilized as a chromosome II marker. GFP expressing non-Vab F2 animals were isolated. Homozygous *rrf-3(pk1426); ezIs2* lines were confirmed by GFP expression analysis and sterility at 25°C (which confirmed the *rrf-3(pk1426)* background).

The *cog-1(sy607); nbIs1000* strain was generated by crossing *cog-1(sy607)/+* males to *nbIs1000* hermaphrodites. F2 Cog Rol animals were isolated and a homozygous *cog-1(sy607); nbIs1000* strain was established. *cog-1(sy607)* homozygotes exhibit extremely low brood sizes but they can be maintained as a homozygous line. This strain was further confirmed by PCR verification of the *cog-1(607)* deletion (Palmer et al., 2002).

Isolation of the *lg6001* deletion allele

A deletion mutant of *nhr-6* was isolated by PCR screening of mutant libraries representing approximately 4,500,000 haploid genomes. Libraries were constructed by trimethylpsoralen treatment in combination with UV irradiation of wild-type N2 animals (Jansen et al., 1997). Subpools were screened for a deletion in the *nhr-6* gene by nested PCR. The first round was performed using primers EG60.1 (5′-TGCTACTCCGCCTTCTCAAT-3′) and EG60.2 (5′-GCTCGATCATTGCACACA-3′), the second round with primers EG60.3 (5′-GACCGCTCATTAATCGGATGCG-3′) and EG60.4 (5′-AGGTTGGTGTGGAGAGGTTG-3′). The isolated *nhr-6(lg6001)* deletion strain (XY1004) was found to be homozygous viable and was outcrossed to N2 five times.

Reverse Transcription-Polymerase Chain Reaction and Western analysis

To identify full-length, SL1 *trans*-spliced *nhr-6* mRNA isoforms 2 μg of total RNA from mixed-stage N2 cultures was reverse-transcribed using the Protoscript First Strand cDNA Synthesis kit (New England Biolabs) with oligo-dT primer. Primary PCR was performed using 1 μl of cDNA template and a primer corresponding to the SL1 *trans*-splice leader sequence and an *nhr-6* 3′UTR specific primer (5′TTGATATTCGGGGATTGGAA-3′). Secondary PCR was performed using the SL1 primer and a nested *nhr-6* 3′UTR primer (5′-GGGGATTGGAATTCACACAA-3′). PCR products were gel purified and sequenced.

NIH-PA Author Manuscript

NIH-PA Author Manuscript

NIH-PA Author Manuscript

Chicken anti-NHR-6 antibodies were generated by Covance Research Products (Denver, PA) using purified His-tagged NHR-6/LBD antigen. The antibody was affinity purified against the antigen followed by affinity purification against an MBP fusion of the NHR6/LBD. SDS-PAGE was performed using equal amounts of protein from mixed-staged N2 and *nhr-6(lg6001)* nematode cultures. Western blots were probed with primary antibodies followed by HRP-linked anti-chicken secondary antibodies. Blots were washed in Tris-buffered saline containing 0.3% Tween 20 and 0.5% Triton-X prior to adding HRP substrate.

Immunolocalization with anti-NHR-6/LBD was attempted but only gave diffuse, apparently non-specific staining in both wild-type and mutant animals. Several approaches and fixation conditions were attempted. The Western analysis described above required very stringent wash conditions to eliminate background signal and this characteristic of the antibody likely affected the immunolocalization experiments.

nhr-6(lg6001) phenotypic analysis

nhr-6(lg6001) homozygotes are viable but adults degenerate rapidly after production of the first few eggs. Therefore, all microscopic phenotypic analyses (except where specifically noted) of *nhr-6(lg6001)* animals were performed during the young adult stage prior to or soon after the first ovulation.

Construction of an *nhr-6* RNAi vector was previously described (Gissendanner et al., 2004). RNAi was performed using a standard RNAi feeding method (Kamath et al., 2001). Robust *nhr-6* RNAi requires utilizing a strain with enhanced RNAi sensitivity. In this study we utilized the RNAi sensitive mutant *eri-1(mg366)* (Kennedy et al., 2004). Synchronized *eri-1(mg366)* L1 larvae derived from alkaline hypochlorite egg preparation were placed on lawns of HT115 *E. coli* bacteria induced with 1mM IPTG to express *nhr-6* double-stranded RNA. Nematodes were grown on induced bacteria at 20°C until they reached the young adult stage.

Brood count experiments were performed by placing single young adults on brood count plates (plates that contain a narrow strip of OP50 *E. coli* bacteria). Animals were moved every 12-24 hours until egg production stopped or until animals “bagged”, as was frequently observed with *nhr-6(lg6001)* mutants. Each time animals were moved, eggs and larvae were counted. 24 hours after adults were moved, each plate was scored for arrested eggs and viable larvae. The viable larvae counts are reported in Table 1. To assess egg morphology and lethality specifically, groups of young adult animals (see Table 2) were placed on a brood count plate and eggs were collected for 24 hours. Adult animals were removed from the plate after egg collection. Abnormal egg morphology was noted when eggs exhibited small size, round shape or other irregular shapes compared to the normal oval shaped eggs produced by wild-type nematodes. Embryonic lethality was assessed 24 hours after egg collection.

To assess the mating ability of *nhr-6(lg6001)* males, three spontaneously arising young adult *nhr-6(lg6001)* males were removed from a mixed stage culture and mated to 3 *dpy-17(e164) unc-32 (e189)* young adult hermaphrodites. >95% of the F1 progeny were cross progeny.

Phalloidin-staining and myosin heavy chain A (MHCA) and MH27 immunohistochemistry was performed on gonads extruded from young adults. Gonads were extruded in PBS/0.01% tetramisole using 25G needles and collected in 1.5 ml siliconized tubes. Fixation of extruded gonads and subsequent staining using anti-MHCA antibody (monoclonal antibody 5.6, gift from David Miller) were performed exactly as previously described (Rose et al., 1997). For anti-AJM-1 staining, the monoclonal MH27 antibody (Developmental Studies Hybridoma

NIH-PA Author Manuscript

NIH-PA Author Manuscript

NIH-PA Author Manuscript

Bank) was used at 1:50 dilution. For phalloidin-staining, extruded gonads were fixed in 1.25% paraformaldehyde for 10min at room temperature and washed twice in PBS/0.5% Triton-X (PBST). Gonads were stained with 0.165 μM FITC-Phalloidin (Sigma-Aldrich) and 1 μg/ml DAPI for one hour in the dark and then washed twice in PBST.

Construction and analysis of *nhr-6(lg6001); fog-2(q71)* double mutants

nhr-6(lg6001); fog-2(q71) double mutants were constructed by crossing *fog-2(q71)* males to IP1005 (*nhr-6(lg6001); jcIs1)* hermaphrodites. IP1005 was utilized so that spermatheca morphology could be assessed in the double mutants using the AJM-1::GFP marker. L4 F2 progeny from the cross were singled to a large number of NGM plates. Both Rol (indicating presence of *jcIs1)* and non-Rol F2 progeny were selected. Plates were screened for sterile animals the following day. Sterile animals were observed with high magnification to confirm Fog phenotype (absence of sperm and fertilized eggs) and scored for ovulation defects. 34 Fog animals were observed. 12/34 contained a proximal mass of oocytes, consistent with ovulation in the absence of sperm. Single animals with and without ovulation defects were removed and genotyped for the *lg6001* allele by PCR using primers 5′-TGCTCTTTTGTCGCAGCTAA-3′ and 5′-GTTACAAGGCTTCCCCGCTA-3′, which detects both the wild-type and *lg6001* deletion allele. All animals with ovulation defects (ovulation in the absence of sperm associated with a proximal mass of fragmented oocytes and lack of oocyte compaction in the gonad arm) were found to be homozygous for the *nhr-6(lg6001)* allele. Normal Fog animals were either +/+ or *nhr-6(lg6001)/+*.

Reporter gene analysis

Construction and initial analysis of the full-length *nhr-6::GFP* reporter (pCG52) has previously been described (Gissendanner et al., 2004). The pCG52-bearing extrachromosomal array, *nbEx1002,* was integrated using a methylmethane sulfonate-based integration protocol graciously provided by Yinhua Zhang, New England Biolabs (manuscript in preparation). One integrated line (*nbIs1000*) was isolated and this line was outcrossed to N2 three times to generate strain IP1018. This strain exhibited an expression pattern identical to the *nbEx1002* strain, IP1004.

Transcriptional reporter constructs for the three putative regulatory regions (R1-3, corresponding to constructs pCG53-55, see Figure 3) were constructed by PCR amplification of the specified genomic regions using a previously described *nhr-6* genomic clone as template (Gissendanner et al., 2004). Amplified products were cloned into the *Pst*I/*Xma*I (for pCG53 and pCG54) or *Sph*I/*Bam*HI (for pCG55) sites of pPD95.67 (gift from Andy Fire). The following primers were utilized: R1 (5′-CCCAATGATCCGATCTGTTT-3′ and 5′-CACAGCAAAAGCATTGTG-3′); R2 (5′-AGCTGTTCCGGAAGTAGTAAGC-3′ and 5′-CTGAAAATGTTCAGAATTTTAACG-3′); R3 (5′-GTGAGCTCTTTTTCCAAGAAC-3′ and 5′-CTGCAAACTTTCAATTTCAGAC-3′).

Transgenic nematodes were generated by injecting 10 μg/ml reporter and 100 μg/ml pRF4 (Mello and Fire, 1995) for pCG53 and pCG54 and 20 μg/ml reporter and 100 μg/ml pRF4 for pCG55. Two independent transgenic lines were analyzed for each construct. Expression from pCG53-bearing arrays was never observed at any stage of development.

Construction of strains bearing *nhr-6(lg6001)* and *nhr-6(tm870)*

The following *nhr-6(lg6001)* strains were constructed for this study: IP1001 (*nhr-6(lg6001)/qC1 dpy-19(e1259) glp-1(q339)*); IP1005 (*nhr-6(lg6001); jcIs1*[*ajm-1::GFP::GFP + rol-6(su1006)*]); IP1014 (*nhr-6(lg6001); tmIs5*[*lim-7::GFP + rol-6(su1006)*]); DN2 (*nhr-6(lg6001); syIs63*[*cog-1::GFP + unc-119(+)*]); DN6 (*nhr-6(lg6001); nbIs1000*); DN7 (*nhr-6(lg6001); baEx2*[*lis-1::GFP + rol-6(su1006)*]); DN10 (*nhr-6(lg6001);*

NIH-PA Author Manuscript

NIH-PA Author Manuscript

NIH-PA Author Manuscript

unc-26(e205)ced-3(n717); nbIs1000); DN18 (*nhr-6(lg6001)/+; let-502::GFP*); DN19 (*nhr-6(lg6001)/+; mel-11::GFP*). Due to the reduced fecundity of *nhr-6(lg6001)* homozygotes, construction of these strains required utilizing large numbers of *nhr-6(lg6001)* hermaphrodites in the P0 crosses. Typically, 30-40 *nhr-6(lg6001)* L4 hermaphrodites crossed to 30-40 N2 young adult males would generate sufficient numbers of F1 *nhr-6(lg6001)/+* males for subsequent crosses. *nhr-6(lg6001)* homozygotes are recognized in the F2 generation of these crosses by the presence of large numbers of bagging animals. Strains bearing the *nhr-6(lg6001)* allele were confirmed by both phenotypic analysis and single worm PCR using primers to detect the *nhr-6(lg6001)* deletion. For strain DN10, *unc-26(e205)* was used to track the *ced-3(n717)* chromosome in the crosses. Three independent lines were isolated and all failed to suppress the *nhr-6(lg6001)* phenotype.

A balanced *nhr-6(tm870)/ qC1 dpy-19(e1259) glp-1(q339)* strain was generated by the same strategy for *nhr-6(lg6001). nhr-6(lg6001)/ nhr-6(tm870) trans*-heterozygotes were generated by crossing *nhr-6(lg6001)/qC1* males to *nhr-6(tm870)/qC1* hermaphrodites. F1 cross progeny were singled to plates. F1 animals were isolated that exhibited an Nhr-6 phenotype. The brood sizes of these animals was assessed and the parent animals were genotyped by PCR using primers 5′TGCTCTTTTGTCGCAGCTAA-3′ and 5′-AGCTCGATCATTGCACACAG-3′ to distinguish the *lg6001* and *tm870* deletions in a single reaction. Data were used only from confirmed *nhr-6(lg6001)/ nhr-6(tm870) trans*-heterozygotes (14/15 animals tested).

Nuclei Counts

Extruded gonads were DAPI stained after fixation as described above. GFP defined cell counts were performed using between 10 and 12 optical sections though the gonad plane on anesthetized IP1018 (chromosomally integrated *nhr-6::gfp* transgene, *nbIs1000*) and *nhr-6(lg6001); nbIs1000* young adults. Micrographs were taken using a Diagnostic Instruments Spot Cam version 2.3.1.1 (Diagnostic Instruments Inc., MI). Micrographs of both GFP expression and DIC images were generated in 16 bit mono Tiff format and aligned in separate layers using Adobe Photoshop CS2 (Adobe Systems Inc., CA). Areas of GFP expression were defined with an opacity of less than 50%. Nuclei, identified on DIC images within the defined GFP expression area, were marked on a separate layer and counted, excluding those nuclei in the spermathecal valves.

Rescue assays

Rescue constructs bearing wild-type *nhr-6* coding sequence were injected into IP1001 hermaphrodites. Stable transgenic lines were isolated and *nhr-6(lg6001)* homozygotes bearing the rescue arrays were recovered. A previously described *nhr-6* genomic clone, pLH1 (Gissendanner et al., 2004), was injected at a concentration of 1 μg/ml along with 100 μg/ml of pRF4 to generate rescuing array *nbEx1000*. To generate a rescuing construct under control of the R3 (intron 5) promoter, the pLH1 genomic clone was digested with *Bam*HI, end-filled, and then digested with *Blp*I. This removes all coding and regulatory sequences upstream of intron 5 as well as most of intron 5. The remaining fragment was gel-purified and ligated to a *Hind*III (end-filled)/*Blp*I intron 5 fragment from the pCG55 transcriptional reporter construct, thus replacing the intron 5 sequence lost in the first step. The final construct consisted of intron 5 followed by all downstream *nhr-6* genomic sequence. The construct was injected at a concentration of 10 μg/ml along with 100 μg/ml pRF4. Two stable arrays were generated and one array, *nbEx1010,* rescued *nhr-6(lg6001)* homozygotes.

NIH-PA Author Manuscript

NIH-PA Author Manuscript

NIH-PA Author Manuscript

RESULTS

nhr-6 encodes two protein isoforms and is required for normal reproduction

nhr-6 gene structure and phylogenetic placement in the NR4A group has been previously described (Gissendanner et al., 2004; Robinson-Rechavi et al., 2005; Sluder and Maina, 2001). To further characterize the *nhr-6* gene, we performed SL1 RT-PCR and determined that *nhr-6* encodes two mRNA isoforms (α and β), differentiated by alternative SL1 *trans*-splicing (Fig. 1A). The shorter *nhr-6β* lacks the first five exons found in *nhr-6*α and the 5′ end of the shorter isoform is defined by *trans*-splicing of SL1 to exon 6. The shorter isoform encodes an NR4A receptor with a shortened N-terminal A/B domain. Western blot analysis (Fig. 1B) of mixed-stage nematodes reveals the presence of two NHR-6 proteins: NHR-6A, and a smaller protein, NHR-6B. The sizes of the two proteins revealed by the Western analysis is consistent with the predicted sizes encoded by the mRNA isoforms (69kDa for NHR-6A and 53kDa for NHR-6B). An ~20kDa protein is also detected in the Western analysis. However, no *nhr-6* mRNA has been isolated that could code for a protein of this size. One possibility is that the ~20kd band could represent a proteolytic product of the NHR-6 protein.

A deletion allele of *nhr-6*, *lg6001*, was isolated using a PCR-based chemical mutagenesis screen. The *lg6001* allele deletes the 3′ splice site of intron 5, exons 6-8, and the 5′ end of exon 9 (Fig. 1A). This deletion removes coding sequence common to both mRNA isoforms and Western blot analysis demonstrates that NHR-6A and NHR-6B proteins are not expressed in *nhr-6(lg6001)* mutant animals, indicating that *nhr-6(lg6001)* is a molecular null allele (Fig. 1B).

Animals homozygous for *nhr-6(lg6001)* are viable but exhibit severe reproductive defects (Table 1). A component of this reproductive defect is a highly penetrant “bagging” phenotype, where the failure to properly lay eggs results in internal hatching of larvae. 21/35 *nhr-6 (lg6001)* homozygous hermaphrodites scored exhibited a “bagging” phenotype. However, homozygous mutants frequently laid eggs prior to bagging. The number of viable offspring from non-bagging *nhr-6 (lg6001)* homozygous animals ranged from 0-38 (average 7.0 + 12.8). 8/14 non-bagging hermaphrodites failed to produce to viable progeny. Therefore, *nhr-6(lg6001)* mutants have a specific defect in the ability to generate progeny that is not solely due to an egg-laying defect.

Another phenotype of *nhr-6(lg6001)* mutants is abnormal egg morphology (Table 2). Wild-type hermaphrodite eggs have a distinct oval shape (Fig. 2A, A’). However, a majority of eggs laid by *nhr-6(lg6001)* homozygous hermaphrodites exhibit a range of abnormal morphology. Phenotypes ranged from small or round eggs to larger eggs with irregularly shaped borders (Fig. 2B and B’). Of the eggs laid by *nhr-6(lg6001)* homozygous hermaphrodites (n=152 eggs scored), 78% exhibited an abnormal egg morphology phenotype and 34% arrested development prior to hatching (Table 2). Only the most severely abnormal eggs arrested development. Normally shaped eggs and eggs with less severe abnormal morphology completed embryonic development and the hatched larvae were viable (Fig. B’). The reproductive and egg morphology phenotypes were rescued by transgenes bearing wild-type *nhr-6* sequence (Table 1). An additional allele of *nhr-6, tm870,* isolated by the S. Mitani laboratory (http://www.shigen.nig.ac.jp/c.elegans/mutants/DetailsSearch?lang=english&seq=870), also displays the same phenotypes as *lg6001* (data not shown). This allele is an 874 bp deletion that overlaps with *lg6001* (Fig. 1A). *nhr-6(lg6001)/nhr-6(tm870) trans*-heterozygotes display low brood size phenotypes similar to *nhr-6(lg6001)* homozygotes (Table 1). In addition, the brood size and abnormal egg morphology phenotypes are also observed in *nhr-6(RNAi)* animals (Table 1 and Table 2). Therefore, we conclude that the observed phenotypes are due specifically to loss of *nhr-6*

NIH-PA Author Manuscript

NIH-PA Author Manuscript

NIH-PA Author Manuscript

function. Abnormal egg morphology, embryonic arrest and decreased brood size are not observed in *nhr-6(lg6001)/+* hermaphrodites, thus, *lg6001* appears to be fully recessive (Table 2).

nhr-6(lg6001) mutants are defective in spermatheca function and ovulation

Microscopic analysis of *nhr-6(lg6001)* homozygous adult hermaphodites revealed evidence of defective ovulation. In wild-type animals, ovulation involves a series of highly coordinated processes wherein the mature, most proximal oocyte in the gonad arm is moved into the spermatheca where it is fertilized (McCarter et al., 1999). After fertilization, the egg moves into the uterus where early embryonic development occurs prior to egg-laying (Fig. 2C). In *nhr-6(lg6001)* hermaphrodites, the proximal oocyte becomes fragmented during the ovulation process (Fig, 2D). Oocyte fragments were frequently observed in the proximal gonad arm (fragmented oocytes are not observed in regions distal to the most proximal oocyte), spermatheca, and uterus. Many fragments are fertilized and form an egg shell, indicating that the basis of the abnormal egg morphology phenotype is oocyte fragmentation and subsequent fertilization. 76% of *nhr-6(lg6001)* adult hermaphrodite gonads contained fragmented oocytes (n=25) when observed soon after mature oocytes begin to ovulate. Endomitotic oocytes are also observed in *nhr-6(lg6001)* gonad arms, further indicating that the ovulation process has been disrupted (Fig. 2E) (McCarter et al., 1999). Older *nhr-6(lg6001)* hermaphrodites display massive degeneration of gonad tissue (Fig. 2E). The basis for the degeneration is unknown. Tissue degeneration and the clogging of the gonad passages by oocyte fragments would ultimately prevent normal gonad function, including egg-laying, and would likely contribute to the bagging phenotype observed in *nhr-6(lg6001)* hermaphrodites.

Observations of ovulation in live *nhr-6(lg6001)* animals revealed that portions of ovulated oocytes often exit the spermatheca and re-enter the gonad arm. This process is likely to lead to oocyte fragmentation and subsequent initiation of endomitosis (McCarter et al., 1997). In addition, developing embryos are often observed within the gonad arm or spermatheca (Fig. 2E, G). 36% of *nhr-6(lg6001)* young adult hermaphrodites displayed this phenotype (n=25). The proportion of animals displaying misplaced developing embryos is increased in older hermpahrodites. Misplacement of developing embryos in the gonad arm or spermatheca and the re-entry of ovulated oocytes back into the gonad arm suggest that the proximal spermatheca valve and the distal spermatheca constriction do not function normally in *nhr-6(lg6001)* mutants. In fact, a spermatheca-uterine valve is not formed in *nhr-6(lg6001)* mutants (see below and Fig. 9). Both the proximal valve and distal constriction must open to allow passage of fertilized eggs and mature oocytes, respectively (see Fig. 5). The opening of these structures is tightly regulated and coordinated with the ovulation process (McCarter et al., 1999).

In addition to the absence of a spermatheca-uterine valve, the distal spermatheca constriction may also not function properly in *nhr-6(lg6001)* hermaphrodites. Ablation of cells in the distal constriction leads to fragmentation of oocytes (McCarter et al., 1997), similar to the fragmentation phenotype of *nhr-6* mutants. Further evidence of abnormal distal spermatheca function was observed in feminized *nhr-6(lg6001); fog-2(q71)* adults. *fog-2(q71)* homozygous mutants are feminized and fail to generate sperm (Schedl and Kimble, 1988). Since ovulation is dependent on sperm signaling (Miller et al., 2001), oocytes in *fog-2(q71)* females are not ovulated or are ovulated at a decreased rate. The lack of ovulation in *fog-2(q71)* females leads to a compaction of oocytes in the ovary (Fig. 3A). *fog-2(q71)* adult females typically only display 1 or 2 unfertilized oocytes in the uterus. In contrast, all early *nhr-6(lg6001); fog-2(q71)* adult females contained a large mass of fragmented oocytes in the spermatheca and uterus (n=12; Fig. 3B). In addition, the compaction of oocytes within the

NIH-PA Author Manuscript

NIH-PA Author Manuscript

NIH-PA Author Manuscript

gonad arm was not observed in these animals, indicating that oocytes were not contained in the gonad arm in the absence of sperm.

The *nhr-6(lg6001); fog-2(q71)* phenotype could be due to either a function for *nhr-6* in the negative regulation of ovulation or to defective morphology of the distal constriction, which would also lead to a lack of oocyte containment. To assess spermatheca morphology, we performed *nhr-6* RNAi in animals bearing an integrated *fkh-6::GFP* transgene (RNAi was necessary as the transgene is integrated into chromosome III, the same chromosome containing the *nhr-6* locus). *fkh-6* is a forkhead transcription factor that regulates sexual identity in *C. elegans* (Chang et al., 2004). *fkh-6::GFP* is expressed strongly in the developing and adult spermatheca (Chang et al., 2004). An RNAi sensitized *rrf-3(pk1426);fkh-6::GFP* was constructed and these animals were subjected to *nhr-6* RNAi. Strongly affected animals (n=10) displayed severe defects in spermatheca morphology. These defects included decreased organ size, misplaced spermatheca nuclei, and a general disorganization that varied from animal to animal (Fig. 4B). Thus, it appears that abnormal spermatheca structure is a likely contributor to the defective ovulation and oocyte fragmentation phenotype. The expression of *fkh-6::GFP* indicates the spermatheca in *nhr-6* loss of function animals is specified properly and that *nhr-6* is not required for *fkh-6::GFP* expression.

Structure of the *C. elegans* spermatheca

The adult *C. elegans* spermatheca is composed of 24 epithelial cells (Lints and Hall, 2006). The apical surfaces of the epithelial cells face a lumen that expands as oocytes enter to become fertilized during ovulation. The lumen also stores mature sperm in gravid adults. The distal part of the spermatheca consists of eight cells that have a shape distinct from the cells that comprise the main part of the expandable sac (Fig. 5A). These specific cells make up a distal constriction that separates the gonad arm from the spermatheca. The cells of the distal constriction and sac contain a distinct pattern of circumferentially oriented actin filaments that allow the cells to expand during ovulation (McCarter et al., 1997). Another important feature of the *C. elegans* spermatheca is the spermatheca-uterine valve. At the young adult stage the valve constists of two syncytial structures. One structure is a 4-cell syncytial toroid that forms a tight, actin filament-rich valve separating the spermatheca from the uterus (Lints and Hall, 2006). Eggs fertilized in the spermatheca must pass through this valve structure to enter the uterus for further development. Another component of the valve is the spermatheca-uterine junction core. This syncytial structure contains two nuclei, the sujc, derived from the uterine lineages. In young adults, the sujc nuclei reside in the distal part of the uterus and extend filopodia through the spermatheca-uterine valve toroid into the spermatheca (Lints and Hall, 2006). The valve core is thought to be lost after the first egg passes from the spermatheca into the uterus. The precise function of the syncytial valve core is not known, although ablation of the sujc in L4 animals leads to reproductive defects (Palmer et al., 2002).

Each spermatheca is derived from two distinct cell lineages (Kimble and Hirsh, 1979). Eighteen of the 24 cells derive from the granddaughter cell of two SS cells. The SS cells are part of the early somatic gonad primordium and the daughters of these cells give rise to the gonad sheath and the distal and sac regions of the spermatheca (Kimble and Hirsh, 1979). The remaining six spermatheca cells are derived from the dorsal uterine (DU) lineage (Z1.papaa and Z4.apaaa for the anterior spermatheca; Z1.pappp and Z4. apapp for the posterior spermatheca). The sujc are also derived from these lineages (Fig. 5B). The sujn derive from a different dorsal uterine lineage.

NIH-PA Author Manuscript

NIH-PA Author Manuscript

NIH-PA Author Manuscript

nhr-6 is expressed in the developing somatic gonad and chemosensory neurons

To determine the expression pattern of *nhr-6*, we examined transgenic animals bearing a previously described *nhr-6::GFP* reporter construct (pCG52 (Gissendanner et al., 2004)) (Fig. 6). This transgene was chromosomally integrated and transgenic nematodes were analyzed at all developmental stages. As previously described for the extrachromosomal array containing this transgene (Gissendanner et al., 2004), we identified *nhr-6::GFP* expression in the integrated line in two cell types: a subset of somatic gonad cells in the L3 and L4 stages (Fig. 7) and a pair of head chemosensory neurons (likely to be ASI based on position) (Fig. 8). *nhr-6::GFP* was also weakly expressed in intestine in late embryos and L1 stage larvae (data not shown). Chemosensory neuron expression was first observed in three-fold embryos and was present in all larval stages and adults. The somatic gonad cells that express GFP in L4 animals include the developing spermatheca cells of the anterior and posterior spermathecae.

nhr-6 is expressed in the developing spermatheca and sujc

A more detailed analysis of developmental expression of *nhr-6::*GFP revealed initial somatic gonad expression in late L3 stage animals in 8 cells of the dorsal somatic gonad primordium (Fig. 7A, B). The positions are consistent with the cells being daughters of the DU and SS somatic gonad founder cells. We have not confirmed that the 8 initial cells that express *nhr-6::GFP* are the specific DU and SS daughter cells that give rise to the spermatheca. However, these GFP expressing cells increase in number and by early L4 they form two groups of cells that will later become the anterior and posterior spermathecae (Fig. 7C, D). The expression in the developing spermathecae continues throughout the L4 stage (Fig. 7E, F). Two cells in the proximal ends of each spermatheca display the brightest expression (Fig. 7E). These cells are the uterine lineage-derived sujc that form the core of the spermatheca-uterine valve (Kimble and Hirsh, 1979). *nhr-6::GFP* is not expressed in the sujn toroidal cells. During the L4/adult molt, expression in the spermatheca diminishes dramatically and in early adults only weak expression is observed in the differentiated sujc cells (Fig. 7G, H). No expression is observed in any spermatheca cells of gravid adults. The GFP expression patterns are also consistent with *nhr-6 in situ* hybridization data from the Y. Kohara laboratory (http://nematode.lab.nig.ac.jp/db2/ShowCloneInfo.php?clone=337g1).

Based on position and developmental stage, the cells that express *nhr-6::GFP* in the late L3 stage are likely to be SS and DU descendents that become spermatheca founder cells. Therefore, *nhr-6::GFP* appears to be expressed at the earliest stages of spermatheca development. The continued expression of *nhr-6::GFP* in the developing spermatheca, and the rapidly diminished expression of the reporter in late L4 suggests that *nhr-6* has a developmental role in spermatheca function.

The function of *nhr-6* in the somatic gonad appears to be specific to hermaphrodites. *nhr-6::GFP* expression was never observed in the developing and adult somatic gonad of male transgenics. Only head neuron expression was observed in males. Gonadal morphology of *nhr-6(lg6001)* mutant males was grossly normal and mutant males were capable of mating and generating cross progeny (see Materials and Methods).

The NHR-6B isoform is sufficient for spermatheca development

To further understand the regulation of *nhr-6* expression, a series of transcriptional reporter fusions were constructed from three regions that could contain important regulatory elements. We have designated these putative regulatory regions R1, R2, and R3 corresponding to DNA sequence upstream of exon 1, exon 2 (intron 1) and exon 6 (intron 5), respectively (Fig. 6). Sequence from intron 1, immediately upstream of exon 2, was selected due to the large size of this intron, suggesting that it could contain regulatory

NIH-PA Author Manuscript

NIH-PA Author Manuscript

NIH-PA Author Manuscript

elements. A reporter construct containing the first half of intron 1 was not constructed so we were unable to determine if regulatory elements reside in this part of the intron. We also reasoned that intron 5 could contain the regulatory elements necessary for expression of the *nhr-6β* isoform since intron 5 is fairly large (~1.8 kb) and lies immediately upstream of the SL1 splice site that defines the 5′ end of *nhr-6β*. We fused these potential regulatory regions to *GFP* and examined their expression patterns in transgenic animals. Expression of *nhr-6R1::GFP* was not observed in any cell type in two independent lines. *nhr-6R2::GFP* expression was observed in chemosensory neurons and the gut, but not in the developing or adult spermatheca. The *nhr-6R3::GFP*, however, was expressed in the developing spermatheca and sujc cells in a pattern identical to that of the original full-length reporter (Fig. 7I ,J). These data indicate that the important regulatory elements required for the spermatheca and sujc expression of *nhr-6* reside in intron 5 of the gene. The alignment of *nhr-6* sequence to the predicted *nhr-6* ortholog in *C. briggsae* (*C. briggsae* predicted gene CBG09761), suggests that intron 5 of *nhr-6* is conserved in *C. briggsae* (data not shown). Conserved blocks of sequence can be identified in this intron in sequence comparisons between *nhr-6* and CBG09761 (Fig. 6).

Based on these results, we hypothesized that NHR-6B is the primary form expressed in the spermatheca. To further address this, we generated a rescue construct that only contains intron 5 and the downstream gene sequence of the shorter NHR-6B isoform. This construct fully rescued the reproductive phenotypes of *nhr-6(lg6001)* mutants (Table 1 and Table 2). This result demonstrates that the NHR-6B isoform, and the putative regulatory elements in intron 5 (and potentially in other downstream introns), are sufficient for normal spermatheca development. In addition, RNAi directed against the specific sequences of the longer *nhr-6*α mRNA isoform failed to generate any reproductive phenotypes (data not shown). Taken together, these data suggest a primary function for NHR-6B during spermatheca development but do not preclude expression or function of the larger isoform in the spermatheca.

We also tested auto-regulation of *nhr-6* expression by crossing the integrated *nhr-6::GFP* into the *nhr-6(lg6001)* mutant background. We found that *nhr-6::GFP* seems to be expressed at normal levels in *nhr-6(lg6001)* mutants, suggesting that *nhr-6* does not autoregulate in the developing spermatheca (Fig. 7K,L). However, bright sujc expression was not observed and the sujc were often found to be mislocalized in the gonad (Fig. 7K,L).

nhr-6 is required for proliferation of the spermatheca lineage

We made several observations of decreased spermatheca organ size (Fig. 4B, and Fig. 9D (below)) in *nhr-6(lg6001)* mutants. To determine if the decreased organ size was due to decreased number of cells, we performed several experiments to quantify spermatheca cell number in *nhr-6* loss of function animals. In wild-type hermaphrodites at the young adult stage the spermatheca nuclei are easy to distinguish from other somatic gonad nuclei with DIC microscopy. However, since *nhr-6(lg6001)* hermaphrodites lack a spermatheca-uterine valve the border between the spermatheca and uterus is not easily distinguishable, limiting the usefulness of DIC analysis of young adult animals to count nuclei. Thus, alternative approaches were utilized. Spermatheca nuclei were first quantified using DAPI staining of extruded spermathcae. This analysis demonstrated that *nhr-6(lg6001)* spermathecae contain ~1/2 the normal number of spermatheca nuclei (Table 3). However, we found it difficult to obtain intact *nhr-6(lg6001)* spermathecae from the extrusion process, probably from the lack of organ integrity in the mutants. To further confirm the spermatheca cell number phenotype of *nhr-6 (lg6001)* we took advantage of the expression of *nhr-6::GFP* in *nhr-6(lg6001)* mutants. For this analysis, we used the *nhr-6::GFP* expression to outline to spermatheca organ in *nhr-6(lg6001)* in mid-late L4 hermaphrodites (spermatheca cell divisions are completed by this stage of development). Using optical sectioning, we then counted the

NIH-PA Author Manuscript

NIH-PA Author Manuscript

NIH-PA Author Manuscript

spermatheca nuclei within the *nhr-6::GFP* expressing region (*nhr-6::GFP* has diffuse cellular expression). This analysis confirmed the decreased cell number phenotype of ~1/2 the normal number of spermatheca nuclei (Table 3). In addition, nuclei counts in young adults from the *rrf-3(pk1426);fkh-6::GFP; nhr-6(RNAi)* experiments further confirmed the cell number defect (Table 3).

The mammalian NR4A NR, Nur77, has been shown to have anti-apoptotic (pro-survival) properties (Suzuki et al., 2003). Therefore, one possibility is that the decreased cell number phenotype we observe could be due to apoptosis of spermatheca cells arising from the lack of *nhr-6* activity in *nhr-6(lg6001)* mutants. Two observations argue against this possibility. First, we were unable to identify apoptotic (nor necrotic) cells in a detailed developmental analysis of spermathecae in *nhr-6(lg6001)* mutants (n=20, data not shown). Second, we constructed *nhr-6(lg6001); ced-3(n717)* double-mutants to genetically prevent apoptosis from occurring in *nhr-6(lg6001)* animals. *nhr-6(lg6001); ced-3(n717)* double-mutants were not suppressed for the reproductive defects (data not shown) nor the cell number defects (Table 3). Therefore, we conclude that *nhr-6* is required for promoting cell proliferation of the spermatheca lineages, rather than preventing cell death, during spermatheca development.

nhr-6 is required for differentiation of the spermatheca

In *nhr-6(lg6001)* mutants the cells that form the spermatheca are specified but exhibit severe differentiation defects. In particular, *nhr-6(lg6001)* spermathecae have a disorganized cellular structure with a more random orientation of actin microfilaments, as indicated by staining with FITC labeled phalloidin (Fig. 9A,B). In addition, the distal constriction does not exhibit the constricted morphology seen in wild-type spermathecae (Fig. 9B).

To specifically assess epithelial differentiation in *nhr-6(lg6001)* spermathecae, we examined the expression of the AJM-1::GFP marker in wild-type and mutant nematodes. The *ajm-1* gene encodes an adhesion junction molecule that is localized to adherens junctions of *C. elegans* epithelia, including the spermatheca (Aono et al., 2004; Koppen et al., 2001). In wild-type animals, the expression of AJM-1::GFP marks the apical, lateral, and basal cell junctions of spermatheca (Lints and Hall, 2006). Apical localization of AJM-1::GFP allows the visualization of the spermathecal lumen that connects the gonad arm to the spermatheca-uterine valve (Fig. 9C). In *nhr-6(lg6001)* mutants, the AJM-1::GFP marker is expressed, again demonstrating that spermathecal cells are specified in *nhr-6(lg6001)* mutants. A lumen can be observed in *nhr-6(lg6001)* mutants, as well as strong punctuate staining associated with AJM-1::GFP localization at the adherens junctions. The lumen of *nhr-6(lg6001)* spermatheca was smaller than wild-type, consistent with other observations of small spermathecae in *nhr-6(lg6001)* mutants (Fig. 9D). However, the expression of AJM-1::GFP was disorganized, and this disorganization was variable from animal to animal. The disorganization likely reflects cellular disorganization of the spermatheca in *nhr-6(lg6001)* mutants as cells of wild-type spermathecae have a highly ordered arrangement ((Lints and Hall, 2006) that is not observed in the mutant animals. Staining of extruded gonads with the monoclonal antibody MH27 (which recognizes the AJM-1 protein) revealed additional cellular defects in *nhr-6(lg6001)* mutants (Fig. 9F). These defects included cells that were either smaller or larger than wild-type spermathecae and a diffuse mislocalization of AJM-1 protein on the basal side of the cells. These phenotypes suggest specific differentiation defects in the spermathecal cells of *nhr-6(lg6001)* mutants.

The spermatheca and another somatic gonad structure, the gonadal sheath that surrounds the gonad, both derive from a common precursor cell, the SS cell. Two SS cells give rise to the gonadal sheath and the majority of the spermatheca cells of each gonad arm. Therefore, one possibility for the observed epithelial defects in *nhr-6 (lg6001)* mutants could be a partial

NIH-PA Author Manuscript

NIH-PA Author Manuscript

NIH-PA Author Manuscript

misspecification (but not complete misspecification as spermatheca markers are expressed in the *nhr-6(lg6001)* hermaphrodites) of spermatheca cells to gonadal sheath cells. This does not appear to be the case as the spermatheca cells of *nhr-6 (lg6001)* animals fail to express myosin, a characteristic of the myoepithelial structure of the gonadal sheath (McCarter et al., 1997) (Fig. 10) as well as *lim-7::GFP*, a sheath-specific marker (Hubbard and Greenstein, 2000) (data not shown). Taken together, these data demonstrate a requirement for *nhr-6* in the proper differentiation, but not specification, of the spermatheca organ. The morphology of the gonadal sheath, as well as the uterus, vulva, and ovary appear grossly normal in developing and young adult *nhr-6(lg6001)* mutants.

Another striking feature of the *nhr-6(lg6001)* phenotype is the completely penetrant absence of a spermatheca-uterine valve (Fig. 9C, D). Apparently, a connection between the spermatheca and the uterus can sometimes form in *nhr-6(lg6001)*; however, this connection does not functionally separate the spermatheca and uterus as highly developed embryos are often observed in the spermatheca of *nhr-6(lg6001)* hermaphrodites (Fig. 2E).

The four cells that make up the valve derive from the uterine cell lineages and these cells have never been observed to express *nhr-6::GFP*. However, in young adults (prior to the first ovulation), these valve cells are closely associated with the sujc syncytium that forms the core of the valve. As noted above, *nhr-6* is expressed in the sujc. A role for the sujc in the formation of the spermatheca-uterine valve has not been formally established. Nonetheless, one possibility for the observed absence of the spermatheca-uterine valve may be a cell nonautonomous role for *nhr-6* in the development of the spermatheca-uterine valve.

nhr-6 is required for the restricted spermathecal expression pattern of *let-502*

The epithelial and cytoskeletal defects associated with *nhr-6* mutant spermathecae suggest that NHR-6 may be required for the normal expression of specific spermatheca differentiation genes. Very few genes have been described that have spermatheca development functions. Two of these genes are *let-502* and *mel-11*. *let-502* and *mel-11* encode a Rho-associated kinase and myosin phosphatase regulatory subunit, respectively (Wissmann et al., 1999). These two proteins have counteracting functions in mediating rearrangements of the actin cytoskeleton. In the spermatheca, *let-502* and *mel-11* have non-overlapping domains of expression (Wissmann et al., 1999). *let-502::GFP* expression is restricted to the distal spermatheca and spermatheca-uterine valve while *mel-11::GFP* is specifically expressed in the spermathecal sac. To determine if the normal expression of these two genes requires *nhr-6* function, we crossed the *let-502::GFP* and *mel-11::GFP* transgenic arrays (a generous gift from Paul Mains, University of Calgary) into the *nhr-6(lg6001)* background. We were unable to generate homozygous *nhr-6(lg6001)* animals bearing the *let-502::GFP* and *mel-11::GFP* transgenic arrays. Therefore, to observe expression of the transgene in animals lacking *nhr-6* function we selected young adult transgenics segregated from *nhr-6(lg6001)/+*; *Ex (*extrachromosomal array bearing *let-502::GFP* or *mel-11::GFP*) animals. Homozygous *nhr-6(lg6001)* young adults were identified at high-magnification by screening for animals that lacked a spermatheca-uterine valve. Both markers were expressed in *nhr-6(lg6001)* mutants (Fig. 11). However, the *let-502::GFP* was misexpressed. Instead of expression being restricted to the distal and proximal regions of the spermatheca, *let-502::GFP* was expressed in all cells of the spermatheca organ in *nhr-6(lg6001)* young adults (n=7 spermathecae; Fig. 11A, B).

mel-11::GFP was normal in *nhr-6(lg6001)* mutants (restricted to the spermatheca sac). GFP expressed from the *mel-11::GFP* transgene is more tightly localized to spermathecal nuclei and, interestingly, and consistent with previous observations, the expression of *mel-11::GFP* was able to reveal a decreased number of spermathecal sac nuclei in *nhr-6(lg6001)* mutants. While the normal 16 spermathecal sac nuclei expressed the marker in wild-type

NIH-PA Author Manuscript

NIH-PA Author Manuscript

NIH-PA Author Manuscript

mel-11::GFP transgenics (as determined by the presence of a normal spermatheca-uterine valve), only 8 + 1 GFP-expressing nuclei (range 7-10; n=6 spermathecae) were observed in *nhr-6(lg6001)* transgenics. In addition, one or more spermathecal nuclei distal to the expressing nuclei were consistently observed not to express GFP. Therefore, as in wild-type spermathecae, *mel-11* also appears to have a proximally-directed expression in *nhr-6(lg6001)* mutants.

These data suggest that *nhr-6* has a specific function in generating domains of *let-502* gene expression important for spermatheca morphogenesis. This is potentially interesting given the apparent distal spermatheca defects of *nhr-6(lg6001)* spermathecae. Loss of proximal-distal polarity, as revealed by the *let-502::GFP* expression, could be a basis for distal defects. However, the alteration in *let-502::GFP* expression can also be explained by the cell proliferation phenotype of *nhr-6(lg6001)* spermathecae. As shown in Fig. 5, most of the spermatheca cells are derived from the SS lineage, including all of the cells of the distal constriction and the distal portion of the spermatheca sac. Therefore, the reduced number of distal cells in *nhr-6(lg6001)* spermatheca may contribute to the apparent loss of restriction in the expression of *let-502::GFP*.

nhr-6 is required for differentiation of the spermatheca-uterine junction core cells

Given the absence of the spermatheca-uterine valve in *nhr-6(lg6001)* mutants, and the expression of *nhr-6::GFP* in the sujc cells that form the core of the valve, we assessed the formation and differentiation of the sujc cells in *nhr-6(lg6001)* animals using *cog-1::GFP* as a specific sujc marker. *cog-1* encodes the *C. elegans* homolog of the Nkx6.1 homeobox transcription factor (Palmer et al., 2002). Like *nhr-6, cog-1* mutants lack spermatheca-uterine valves (in addition to other gonad defects). We crossed an integrated *cog-1::GFP* reporter into the *nhr-6(lg6001)* background and assessed *cog-1::GFP* expression in 30 sets of sujc syncytia at the late L4 or young adult stage. Expression of *cog-1::GFP* was seen in 28/30 sets of sujc cells. 19 of these 28 displayed the normal number of 2 expressing sujc nuclei. Only one expressing sujc nucleus was seen in the remaining 9 sujc observations. *cog-1::GFP* expressing sujc cells were frequently misplaced in the somatic gonad and all sujc cells displayed differentiation defects. The level of *cog-1::GFP* expression was also frequently decreased. In young wild-type adults, the two nuclei of the sujc syncytium are found in the lumen of the uterus and filopodia extend across the valve lumen into the spermatheca (Fig. 12A). In *nhr-6(lg6001)* mutants, this normal morphology was never observed (Fig. 12B). Similar results were obtained with another sujc marker, *lis-1::GFP* (Dawe et al., 2001) (data not shown). Alterations in sujc formation and differentiation were never observed in *nhr-6(+)* hermaphrodites (n=30). These data indicate a function for *nhr-6* in the differentiation, and possibly the specification, or generation, of the sujc syncytium.

Since *cog-1* also encodes a transcription factor, we were interested in whether *nhr-6* expression requires *cog-1*. We crossed the integrated *nhr-6::GFP* transgene into the *cog-1(sy607)* mutant background. Interestingly, we did not observe *nhr-6::GFP* expression in the proximal region of the spermatheca (Fig. 12C,D). In wild-type animals, bright expression of *nhr-6::GFP* is observed in the proximal spermatheca in the cells that form the sujc (see Fig. 7E). Expression of *nhr-6::GFP* in the spermatheca proper was not affected. While this result supports an upstream role for *cog-1* in the regulation of *nhr-6::GFP* expression, we were not able to confirm if the sujc are formed in *cog-1(sy607)* mutants. Thus, the loss of expression could be due to absence of the sujc as opposed to a specific loss of *nhr-6::GFP* expression. Intron 5 of *nhr-6* does contain several TAAT-containing sequence elements that are similar to vertebrate Nkx6.1 binding sites (Jorgensen et al., 1999; Mirmira et al., 2000), and these could function as COG-1 homebox binding sites (data not shown).

NIH-PA Author Manuscript

NIH-PA Author Manuscript

NIH-PA Author Manuscript

DISCUSSION

NR4A is necessary for normal reproduction in *C. elegans*

We have demonstrated that the *C. elegans* NR4A nuclear receptor, *nhr-6,* is an essential gene for reproduction. Two mRNA and protein isoforms are expressed from the *nhr-6* gene. The isoforms differ in the size of the N-terminal A/B domain and both would be expected to be able to bind DNA and activate transcription. Nematodes homozygous for a molecular null allele of *nhr-6*, *lg6001,* exhibit significantly reduced brood sizes and lay eggs that have abnormal morphology and frequently arrest development. The decreased brood size and abnormal egg morphology (and embryonic lethality) appear to arise from defective oocyte ovulation that results in the fragmentation of oocytes. This ovulation defect is a likely secondary consequence of abnormal spermatheca development. *nhr-6* is expressed in the developing spermatheca and *nhr-6(lg6001)* mutants display an abnormal spermatheca morphology that would preclude normal ovulation. A striking feature of the *nhr-6(lg6001)* spermathecae is the absence of a proximal valve and morphologically abnormal distal constriction. The proximal valve and distal constriction have important roles in functionally separating the spermatheca from the uterus and ovary, respectively. This lack of separation likely prevents the ovulation process from being completed properly due to the ability of ovulated oocytes to re-enter the ovary. The lack of a spermatheca-uterine valve often leads to developing eggs residing in the spermatheca. Such situations would likely halt the reproductive process and lead to the “bagging” phenotype observed in mutant hermaphrodites.

We found that the shorter NHR-6 isoform, NHR-6B, is sufficient to direct normal spermatheca development. The N-terminal A/B domain has been shown to be important for the activity of NR4A NRs (Nordzell et al., 2004; Paulsen et al., 1992; Wansa et al., 2002). Since NR4A NRs appear to be true orphan receptors, post-translational modification of the A/B domain is likely to be critical in regulating NR4A activity. Rescue by the NHR-6B isoform identifies the C-terminal half the NHR-6 A/B domain as potentially important for NHR-6 activity. We also determined that the important regulatory elements driving *nhr-6* expression in the spermatheca are found in the 1.8 kb intron 5, which lies directly upstream of the SL1 splice site that defines the beginning of *nhr-6β*. This intron appears to be conserved in *C. briggsae* and contains conserved blocks of sequence. This will facilitate the identification of upstream regulators of *nhr-6.*

Regulation of cell proliferation by NHR-6

In some contexts NR4A NRs have been shown to have mitogenic properties (Kolluri et al., 2003; Maxwell and Muscat, 2006; Nomiyama et al., 2006; Ponnio et al., 2002). Our data also suggest a role for NHR-6 in cell proliferation. Using a variety of approaches we have determined that the spermatheca of *nhr-6* mutants have ~1/2 the normal number of cells. Our observations support the notion that the decrease in the number of cells is likely due to a failure in proliferation and not the activation cell death pathways. There are three possible explanations for the decrease in spermatheca cell number in *nhr-6(lg6001)* mutants. One explanation is not supported by our data: a cell fate transformation from spermatheca to sheath (both of which derive from a common precursor cell). Cell marker analysis demonstrates that the spermatheca is specified properly in *nhr-6* mutants and, additionally, sheath cell markers are not ectopically expressed in mutant spermathecae. However, the cell proliferation defect could still be due to a lineage transformation. In each of the SS lineages that give rise to the spermatheca, the SS granddaughter cell that serves as a spermatheca founder cell undergoes an asymmetric division. As an example, the anterior spermatheca founder cell Z1.paapp divides to generate an anterior and posterior daughter (see Fig. 5B). The posterior daughter cell divides only once more to generate two spermatheca cells while

NIH-PA Author Manuscript

NIH-PA Author Manuscript

NIH-PA Author Manuscript

the anterior daughter cell begins a more proliferative lineage that generates 7 distal spermatheca cells through three rounds of cell division. Thus, the decrease in cell number could be due to a transformation in the SS-derived spermatheca founder cell lineage (anterior→posterior for Z1.paapp). Such a transformation would decrease the number of distal spermatheca cells, leading to the formation of 11 total spermatheca cells (assuming all other divisions occur normally) and would explain the distal constriction morphology defects and the loss of polarity in *let-502::GFP*. The other possibility is that NHR-6 functions as a global regulator of cell proliferation and the observed cell number defect would thus be caused by a failure of cell divisions in all spermatheca lineages (both SS and DU derived). This latter possibility is better supported by the current data since global regulation would likely lead to animal to animal variability in cell number (which we observe) as well as a failure to produce cells from each lineage (which we also observe from the incompletely penetrant loss of sujc cells in *nhr-6 (lg6001)* mutants). Detailed lineage analysis will be required to determine which of these two models is correct.

nhr-6 may have multiple functions during spermatheca development

The epithelial defects of the spermathecae and the cell shape defects and disorganization of spermatheca and the spermatheca-uterine junction core (sujc) cells in *nhr-6(lg6001)* animals suggest strongly a differentiation function for *nhr-6*. Since *nhr-6::GFP* is expressed during the proliferative and differentiation stages of spermatheca development, it is tempting to speculate that *nhr-6* may have dual functions in regulating cell proliferation and cell differentiation, possibly through the regulation of distinct gene sets in response to distinct cell-cell signals. A specific role for *nhr-6* in cellular differentiation is supported by the sujc differentiation phenotype of *nhr-6* mutants. The incompletely penetrant absence of the sujc in *nhr-6(lg6001)* animals indicates that *nhr-6* functions in the generation of these cells. However, even when these cells are generated in *nhr-6(lg6001)* mutants they fail to display normal sujc morphology. Thus, NHR-6 likely functions in the transcriptional regulation of genes that direct sujc differentiation. A dual role for *nhr-6* would be intriguing as it would position NHR-6 as a potential regulator of the cell proliferation to differentiation transition. The regulation of this transition in different organogenesis contexts is still very much an unsolved problem in developmental biology. The exact role of *nhr-6* in spermatheca development will require careful temporal studies of gene function.

NHR-6 has a conserved function in organ development

The organogenesis role for *nhr-6* is consistent with observed functions for NR4A nuclear receptors in vertebrates. NR4A NRs Nurr1 and NOR-1 have established roles in tissue differentiation and organ development, respectively, in mammals. All three NR4A NR paralogs have multiple biological roles in mammalian systems (Maxwell and Muscat, 2006). Despite this functional diversity, a common theme for the NR4A group is emerging. Each of the three mammalian paralogs (Nur77, Nurr1, NOR-1) regulate cell survival, cell proliferation, and/or cell differentiation in different biological processes (Castro et al., 2001; Kolluri et al., 2003; Martinez-Gonzalez et al., 2003; Ponnio et al., 2002; Ponnio and Conneely, 2004; Suzuki et al., 2003; Zeng et al., 2006; Zetterstrom et al., 1997). Nur77 has both pro-apoptotic and anti-apoptotic functions depending on the cellular context (Li et al., 2000; Suzuki et al., 2003). An ancestral function for this group may be the regulation of these cellular activities. The functions described here for *nhr-6* are consistent with this notion. In *C. elegans*, the NHR-6 nuclear receptor appears to be regulating proliferation and differentiation during spermatheca development. Therefore, further studies of NHR-6 should enhance our general understanding of the cellular activities of this NR group.

NIH-PA Author Manuscript

NIH-PA Author Manuscript

NIH-PA Author Manuscript

The *C. elegans* spermatheca as a model system for organogenesis

Our study also illuminates the spermatheca as a new *C. elegans* model for the genetic regulation of organogenesis. The spermatheca has several unique features that argue for its utility as an organogenesis model. First, the spermatheca is a highly secretory organ and functions in signaling processes involving the gonad sheath and oocytes during ovulation (Bui and Sternberg, 2002; Clandinin et al., 1998). Signaling interactions with sperm are also evident as sperm are stored in the adult spermatheca and motile sperm from males preferentially migrate to this organ. In addition to this functional complexity, the spermatheca also exhibits structural complexity. The spermatheca is an endothelial-like tube with regulated valve connections to other tissues (ovary and uterus). This type of organ structure is commonplace in animals and genetic studies in *C. elegans* will provide insight into morphogenetic processes that shape this type of organ.

Our data also further establish the importance of the spermatheca-uterine valve core in organizing the *C. elegans* somatic gonad. It has been reported that the sujc are not generated in *cog-1* mutants and a functional spermatheca-uterine valve fails to develop (Palmer et al., 2002). Likewise, a spermatheca-uterine valve is not generated in *nhr-6(lg6001)* mutants. Like *cog-1, nhr-6* is expressed in the sujc but not in the uterine derived torroidal valve cells. Also, similar to *cog-1* mutants, the sujc in *nhr-6* mutants are either not generated or do not properly differentiate. Thus the transient sujc must have an important role in organizing the valve junction between the uterus and spermatheca, most likely through signaling interactions between the sujc and cells deriving from the uterine lineage. Our GFP reporter epistasis data suggest that NHR-6 functions downstream or in parallel to COG-1. As such, COG-1 is a good candidate to be an upstream regulator of NHR-6 during development of the sujc.

Acknowledgments

We thank David Greenstein, Paul Mains, Guy Caldwell, and Elegene AG (formerly of Martinsreid, Germany) for providing nematode strains; Yinhua Zhang from New England Biolabs for sharing an unpublished array integration protocol; and Brian Rowan for comments on the manuscript. Some strains were provided by the *Caenorhabditis* Genetics Center. This work was partly supported by start-up funds to C.R.G. from the Howard Hughes Undergraduate Education Program at ULM, grant P20 RR16456 under the INBRE Program of the National Center for Research Resources (NCRR), a component of the National Institutes of Health (NIH), and grant LEQSF (2005-2008)-RD-A-39 to C.R.G. from the Louisiana Board of Regents. C.R.G. and C.V.M. gratefully acknowledge the support of Don Comb.

References

Aono S, Legouis R, Hoose WA, Kemphues KJ. PAR-3 is required for epithelial cell polarity in the distal spermatheca of C. elegans. Development. 2004; 131:2865–74. [PubMed: 15151982]

Brenner S. The genetics of Caenorhabditis elegans. Genetics. 1974; 77:71–94. [PubMed: 4366476]

Bui YK, Sternberg PW. Caenorhabditis elegans inositol 5-phosphatase homolog negatively regulates inositol 1,4,5-triphosphate signaling in ovulation. Mol Biol Cell. 2002; 13:1641–51. [PubMed: 12006659]

Castro DS, Hermanson E, Joseph B, Wallen A, Aarnisalo P, Heller A, Perlmann T. Induction of cell cycle arrest and morphological differentiation by Nurr1 and retinoids in dopamine MN9D cells. J Biol Chem. 2001; 276:43277–84. [PubMed: 11553630]

Chang W, Tilmann C, Thoemke K, Markussen FH, Mathies LD, Kimble J, Zarkower D. A forkhead protein controls sexual identity of the C. elegans male somatic gonad. Development. 2004; 131:1425–36. [PubMed: 14993191]

Clandinin TR, DeModena JA, Sternberg PW. Inositol trisphosphate mediates a RAS-independent response to LET-23 receptor tyrosine kinase activation in C. elegans. Cell. 1998; 92:523–33. [PubMed: 9491893]

NIH-PA Author Manuscript

NIH-PA Author Manuscript

NIH-PA Author Manuscript

Dawe AL, Caldwell KA, Harris PM, Morris NR, Caldwell GA. Evolutionarily conserved nuclear migration genes required for early embryonic development in Caenorhabditis elegans. Dev Genes Evol. 2001; 211:434–41. [PubMed: 11685578]

Giguere V. Orphan nuclear receptors: from gene to function. Endocr Rev. 1999; 20:689–725. [PubMed: 10529899]

Gissendanner CR, Crossgrove K, Kraus KA, Maina CV, Sluder AE. Expression and function of conserved nuclear receptor genes in Caenorhabditis elegans. Dev Biol. 2004; 266:399–416. [PubMed: 14738886]

Hubbard EJ, Greenstein D. The Caenorhabditis elegans gonad: a test tube for cell and developmental biology. Dev Dyn. 2000; 218:2–22. [PubMed: 10822256]

Jansen G, Hazendonk E, Thijssen KL, Plasterk RH. Reverse genetics by chemical mutagenesis in Caenorhabditis elegans. Nat Genet. 1997; 17:119–21. [PubMed: 9288111]

Jorgensen MC, Vestergard Petersen H, Ericson J, Madsen OD, Serup P. Cloning and DNA-binding properties of the rat pancreatic beta-cell-specific factor Nkx6. FEBS Lett. 1999; 461:287–94. [PubMed: 10567713]

Kamath RS, Martinez-Campos M, Zipperlen P, Fraser AG, Ahringer J. Effectiveness of specific RNA-mediated interference through ingested double-stranded RNA in Caenorhabditis elegans. Genome Biol. 2001; 2 RESEARCH0002.

Kennedy S, Wang D, Ruvkun G. A conserved siRNA-degrading RNase negatively regulates RNA interference in C. elegans. Nature. 2004; 427:645–9. [PubMed: 14961122]

Kimble J, Hirsh D. The postembryonic cell lineages of the hermaphrodite and male gonads in Caenorhabditis elegans. Dev Biol. 1979; 70:396–417. [PubMed: 478167]

King-Jones K, Thummel CS. Nuclear receptors--a perspective from Drosophila. Nat Rev Genet. 2005; 6:311–23. [PubMed: 15803199]

Kipreos ET. C. elegans cell cycles: invariance and stem cell divisions. Nat Rev Mol Cell Biol. 2005; 6:766–76. [PubMed: 16314866]

Kolluri SK, Bruey-Sedano N, Cao X, Lin B, Lin F, Han YH, Dawson MI, Zhang XK. Mitogenic effect of orphan receptor TR3 and its regulation by MEKK1 in lung cancer cells. Mol Cell Biol. 2003; 23:8651–67. [PubMed: 14612408]

Koppen M, Simske JS, Sims PA, Firestein BL, Hall DH, Radice AD, Rongo C, Hardin JD. Cooperative regulation of AJM-1 controls junctional integrity in Caenorhabditis elegans epithelia. Nat Cell Biol. 2001; 3:983–91. [PubMed: 11715019]

Li H, Kolluri SK, Gu J, Dawson MI, Cao X, Hobbs PD, Lin B, Chen G, Lu J, Lin F, Xie Z, Fontana JA, Reed JC, Zhang X. Cytochrome c release and apoptosis induced by mitochondrial targeting of nuclear orphan receptor TR3. Science. 2000; 289:1159–64. [PubMed: 10947977]

Lints, R.; Hall, DH. Reproductive system, part II. WormAtlas. 2006. http://www.wormatlas.org/handbook/reproductivesystem/reproductivesystem.htm

Maira M, Martens C, Batsche E, Gauthier Y, Drouin J. Dimer-specific potentiation of NGFI-B (Nur77) transcriptional activity by the protein kinase A pathway and AF-1-dependent coactivator recruitment. Mol Cell Biol. 2003; 23:763–76. [PubMed: 12529383]

Mangelsdorf DJ, Thummel C, Beato M, Herrlich P, Schutz G, Umesono K, Blumberg B, Kastner P, Mark M, Chambon P, et al. The nuclear receptor superfamily: the second decade. Cell. 1995; 83:835–9. [PubMed: 8521507]

Martinez-Gonzalez J, Rius J, Castello A, Cases-Langhoff C, Badimon L. Neuron-derived orphan receptor-1 (NOR-1) modulates vascular smooth muscle cell proliferation. Circ Res. 2003; 92:96–103. [PubMed: 12522126]

Maxwell MA, Muscat GE. The NR4A subgroup: immediate early response genes with pleiotropic physiological roles. Nucl Recept Signal. 2006; 4:e002. [PubMed: 16604165]

McCarter J, Bartlett B, Dang T, Schedl T. Soma-germ cell interactions in Caenorhabditis elegans: multiple events of hermaphrodite germline development require the somatic sheath and spermathecal lineages. Dev Biol. 1997; 181:121–43. [PubMed: 9013925]

McCarter J, Bartlett B, Dang T, Schedl T. On the control of oocyte meiotic maturation and ovulation in Caenorhabditis elegans. Dev Biol. 1999; 205:111–28. [PubMed: 9882501]

NIH-PA Author Manuscript

NIH-PA Author Manuscript

NIH-PA Author Manuscript

Mello, C.; Fire, A. DNA transformation. In: Epstein, HF.; Shakes, DC., editors. *Caenorhabditis elegans*: Modern Biological Analysis of an Organism. Vol. Vol. 48. Academic Press; San Diego, CA: 1995. p. 451-482.

Miller MA, Nguyen VQ, Lee MH, Kosinski M, Schedl T, Caprioli RM, Greenstein D. A sperm cytoskeletal protein that signals oocyte meiotic maturation and ovulation. Science. 2001; 291:2144–7. [PubMed: 11251118]

Mirmira RG, Watada H, German MS. Beta-cell differentiation factor Nkx6.1 contains distinct DNA binding interference and transcriptional repression domains. J Biol Chem. 2000; 275:14743–51. [PubMed: 10799563]

Newman AP, Acton GZ, Hartwieg E, Horvitz HR, Sternberg PW. The lin-11 LIM domain transcription factor is necessary for morphogenesis of C. elegans uterine cells. Development. 1999; 126:5319–26. [PubMed: 10556057]

Newman AP, Inoue T, Wang M, Sternberg PW. The Caenorhabditis elegans heterochronic gene lin-29 coordinates the vulval-uterine-epidermal connections. Curr Biol. 2000; 10:1479–88. [PubMed: 11114514]

Nomiyama T, Nakamachi T, Gizard F, Heywood EB, Jones KL, Ohkura N, Kawamori R, Conneely OM, Bruemmer D. The NR4A orphan nuclear receptor NOR1 is induced by platelet-derived growth factor and mediates vascular smooth muscle cell proliferation. J Biol Chem. 2006; 281:33467–76. [PubMed: 16945922]

Nordzell M, Aarnisalo P, Benoit G, Castro DS, Perlmann T. Defining an N-terminal activation domain of the orphan nuclear receptor Nurr1. Biochem Biophys Res Commun. 2004; 313:205–11. [PubMed: 14672718]

Palmer RE, Inoue T, Sherwood DR, Jiang LI, Sternberg PW. Caenorhabditis elegans cog-1 locus encodes GTX/Nkx6.1 homeodomain proteins and regulates multiple aspects of reproductive system development. Dev Biol. 2002; 252:202–13. [PubMed: 12482710]

Paulsen RE, Weaver CA, Fahrner TJ, Milbrandt J. Domains regulating transcriptional activity of the inducible orphan receptor NGFI-B. J Biol Chem. 1992; 267:16491–6. [PubMed: 1644831]

Pekarsky Y, Hallas C, Palamarchuk A, Koval A, Bullrich F, Hirata Y, Bichi R, Letofsky J, Croce CM. Akt phosphorylates and regulates the orphan nuclear receptor Nur77. Proc Natl Acad Sci U S A. 2001; 98:3690–4. [PubMed: 11274386]

Ponnio T, Burton Q, Pereira FA, Wu DK, Conneely OM. The nuclear receptor Nor-1 is essential for proliferation of the semicircular canals of the mouse inner ear. Mol Cell Biol. 2002; 22:935–45. [PubMed: 11784868]

Ponnio T, Conneely OM. nor-1 Regulates Hippocampal Axon Guidance, Pyramidal Cell Survival, and Seizure Susceptibility. Mol Cell Biol. 2004; 24:9070–8. [PubMed: 15456880]

Rajakumar V, Chamberlin HM. The Pax2/5/8 gene egl-38 coordinates organogenesis of the C. elegansegg-laying system. Dev Biol. 2006

Robinson-Rechavi M, Maina CV, Gissendanner CR, Laudet V, Sluder A. Explosive lineage-specific expansion of the orphan nuclear receptor HNF4 in nematodes. J Mol Evol. 2005; 60:577–86. [PubMed: 15983867]

Rose KL, Winfrey VP, Hoffman LH, Hall DH, Furuta T, Greenstein D. The POU gene ceh-18 promotes gonadal sheath cell differentiation and function required for meiotic maturation and ovulation in Caenorhabditis elegans. Dev Biol. 1997; 192:59–77. [PubMed: 9405097]

Schedl T, Kimble J. fog-2, a germ-line-specific sex determination gene required for hermaphrodite spermatogenesis in Caenorhabditis elegans. Genetics. 1988; 119:43–61. [PubMed: 3396865]

Sears RC, Nevins JR. Signaling networks that link cell proliferation and cell fate. J Biol Chem. 2002; 277:11617–20. [PubMed: 11805123]

Sluder AE, Maina CV. Nuclear receptors in nematodes: themes and variations. Trends Genet. 2001; 17:206–13. [PubMed: 11275326]

Sulston JE, Horvitz HR. Post-embryonic cell lineages of the nematode, Caenorhabditis elegans. Dev Biol. 1977; 56:110–56. [PubMed: 838129]

Suzuki S, Suzuki N, Mirtsos C, Horacek T, Lye E, Noh SK, Ho A, Bouchard D, Mak TW, Yeh WC. Nur77 as a survival factor in tumor necrosis factor signaling. Proc Natl Acad Sci U S A. 2003; 100:8276–80. [PubMed: 12815108]

NIH-PA Author Manuscript

NIH-PA Author Manuscript

NIH-PA Author Manuscript

Swanson KD, Taylor LK, Haung L, Burlingame AL, Landreth GE. Transcription factor phosphorylation by pp90(rsk2). Identification of Fos kinase and NGFI-B kinase I as pp90(rsk2). J Biol Chem. 1999; 274:3385–95. [PubMed: 9920881]

Vidwans SJ, Su TT. Cycling through development in Drosophila and other metazoa. Nat Cell Biol. 2001; 3:E35–9. [PubMed: 11146648]

Wang M, Sternberg PW. Pattern formation during C. elegans vulval induction. Curr Top Dev Biol. 2001; 51:189–220. [PubMed: 11236714]

Wang Z, Benoit G, Liu J, Prasad S, Aarnisalo P, Liu X, Xu H, Walker NP, Perlmann T. Structure and function of Nurr1 identifies a class of ligand-independent nuclear receptors. Nature. 2003; 423:555–60. [PubMed: 12774125]

Wansa KD, Harris JM, Muscat GE. The activation function-1 domain of Nur77/NR4A1 mediates trans-activation, cell specificity, and coactivator recruitment. J Biol Chem. 2002; 277:33001–11. [PubMed: 12082103]

Wingate AD, Campbell DG, Peggie M, Arthur JS. Nur77 is phosphorylated in cells by RSK in response to mitogenic stimulation. Biochem J. 2006; 393:715–24. [PubMed: 16223362]

Wissmann A, Ingles J, Mains PE. The Caenorhabditis elegans mel-11 myosin phosphatase regulatory subunit affects tissue contraction in the somatic gonad and the embryonic epidermis and genetically interacts with the Rac signaling pathway. Dev Biol. 1999; 209:111–27. [PubMed: 10208747]

Zeng H, Qin L, Zhao D, Tan X, Manseau EJ, Van Hoang M, Senger DR, Brown LF, Nagy JA, Dvorak HF. Orphan nuclear receptor TR3/Nur77 regulates VEGF-A-induced angiogenesis through its transcriptional activity. J Exp Med. 2006; 203:719–29. [PubMed: 16520388]

Zetterstrom RH, Solomin L, Jansson L, Hoffer BJ, Olson L, Perlmann T. Dopamine neuron agenesis in Nurr1-deficient mice. Science. 1997; 276:248–50. [PubMed: 9092472]

NIH-PA Author Manuscript

NIH-PA Author Manuscript

NIH-PA Author Manuscript

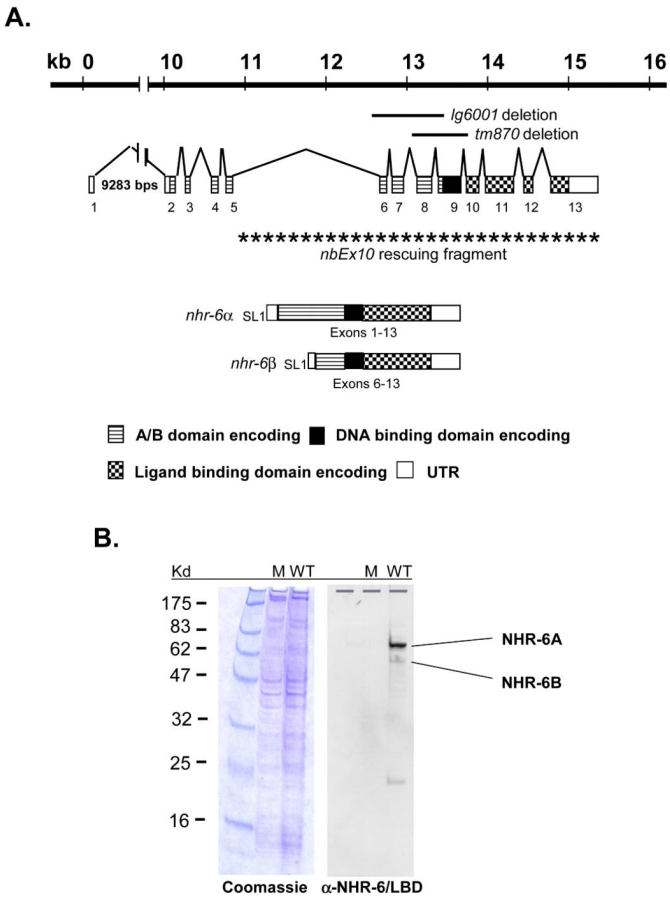

Figure 1. *nhr-6* gene structure and protein expression

(A) Structure of the *nhr-6* gene. The two mRNA isoforms, α and β, are defined by the alternate SL1 *trans*-splice sites. The *nhr-6β* isoform consists of exons 6-13. Exon numbers, the two deletion alleles, and the *nhr-6β* genomic sequence found in the *nbEx10* rescuing array are indicated. (B) Western blot analysis of NHR-6 in wild-type (WT) and *nhr-6(lg6001)* (M) nematodes. NHR-6A and NHR-6B isoforms are indicated. Coomassie stained gel on the left indicates protein loading.

NIH-PA Author Manuscript
NIH-PA Author Manuscript
NIH-PA Author Manuscript

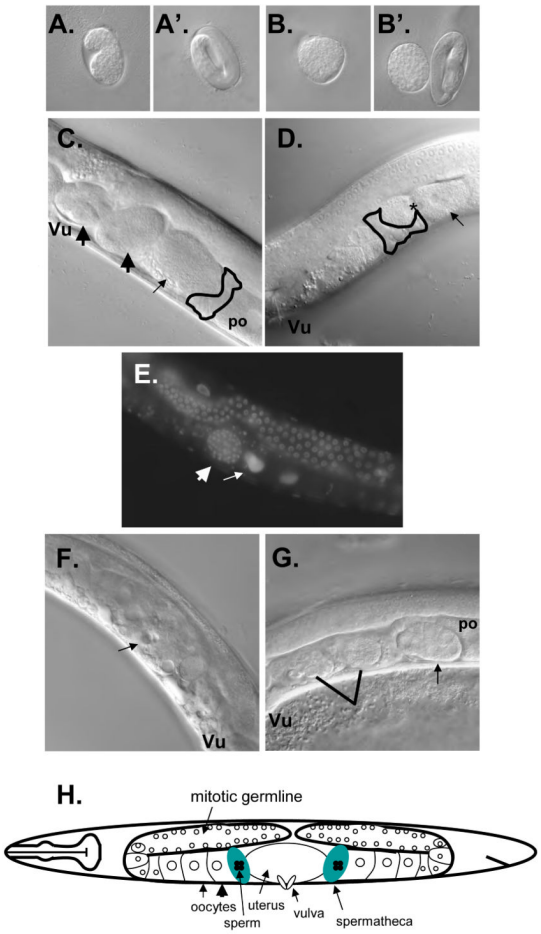

Figure 2. *nhr-6(lg6001)* phenotypes

(A, A') Wild-type egg morphology. (B, B') Typical abnormal egg morphology of *nhr-6(lg6001)* mutants. The embryo in (B) has failed to undergo morphogenesis. Note rounded shape compared to wild-type embryo in (A). The embryo to the right in (B') has developed to the three-fold stage but egg morphology is still abnormal (compare to A'). (C) Wild-type adult hermaphrodite. During ovulation the proximal oocyte (po) is ovulated into the spermatheca (outlined) and is fertilized (thin arrow). Fertilized oocytes then enter the uterus (thick arrows) where they undergo early development prior to being laid through the vulva (Vu). (D) Adult *nhr- 6(lg6001)* hermaphrodite. In this animal the proximal oocyte (thin arrow) is splitting in two during the ovulation process and contains endomitotic nuclei (*). (E) DAPI staining of an *nhr-6(lg6001)* hermaphrodite. Thin arrow indicates the increased, diffuse nuclear DNA staining resulting from endomitosis. Thick arrow indicates a well-developed egg residing within the spermatheca. (F) Older *nhr-6(lg6001)* hermaphrodite displaying gonadal degeneration. (G) *nhr-6 (lg6001)* adult hermaphrodite with misplaced developing embryo. Arrow indicates developing embryo residing in the gonad arm. Also indicated is a split egg with one half in the uterus developing (left) and the other half in the spermatheca that failed to develop (right). (H) Schematic of the *C. elegans* reproductive system.

NIH-PA Author Manuscript
NIH-PA Author Manuscript
NIH-PA Author Manuscript

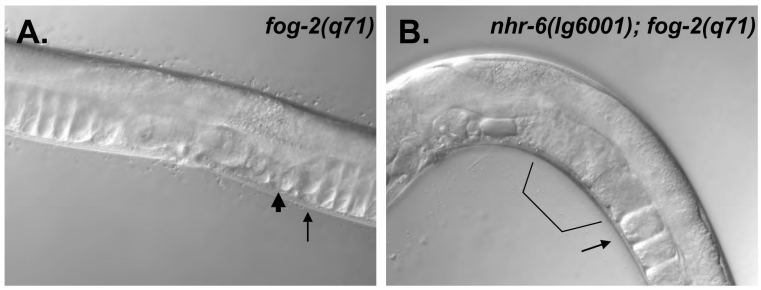

Figure 3. Ovulation in *nhr-6(lg6001); fog-2(q71)* females

DIC micrographs of *fog- 2(q71)* (A) and *nhr-6(lg6001); fog-2(q71)* (B) adults. The spermatheca (thick arrow) and proximal oocyte (thin arrow) are indicated for the animal in (A). Note compaction of the oocytes in the gonad arm (arrow). The animal in (B) lacks the oocyte compaction (arrow) and the proximal gonad is filled with a mass of oocytes and oocyte fragments (bracket).

NIH-PA Author Manuscript

NIH-PA Author Manuscript

NIH-PA Author Manuscript

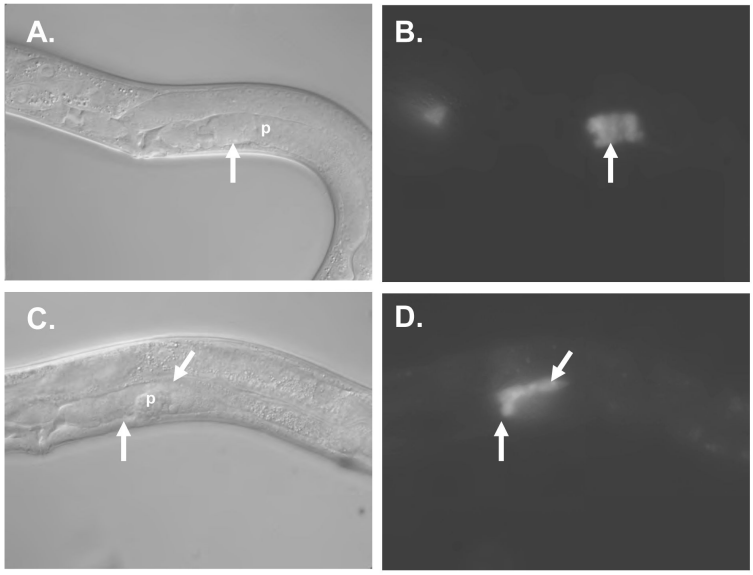

Figure 4. Expression of *fkh-6::GFP* in *nhr-6(RNAi)* hermaphrodites

DIC (A, C) and epifluorescence (B, D) micrographs of *fkh-6::GFP* (A,B) and *fkh-6::GFP; nhr-6(RNAi)* (C, D) young adults. "p" indicates the proximal end of the gonad arm. Arrow indicates the spermatheca. The spermatheca in the *fkh-6::GFP; nhr-6(RNAi)* hermaphrodite is misshapen and spermatheca nuclei are observed over the dorsal side of the gonad arm, indicating loss of normal distal spermatheca organization.

NIH-PA Author Manuscript

NIH-PA Author Manuscript

NIH-PA Author Manuscript

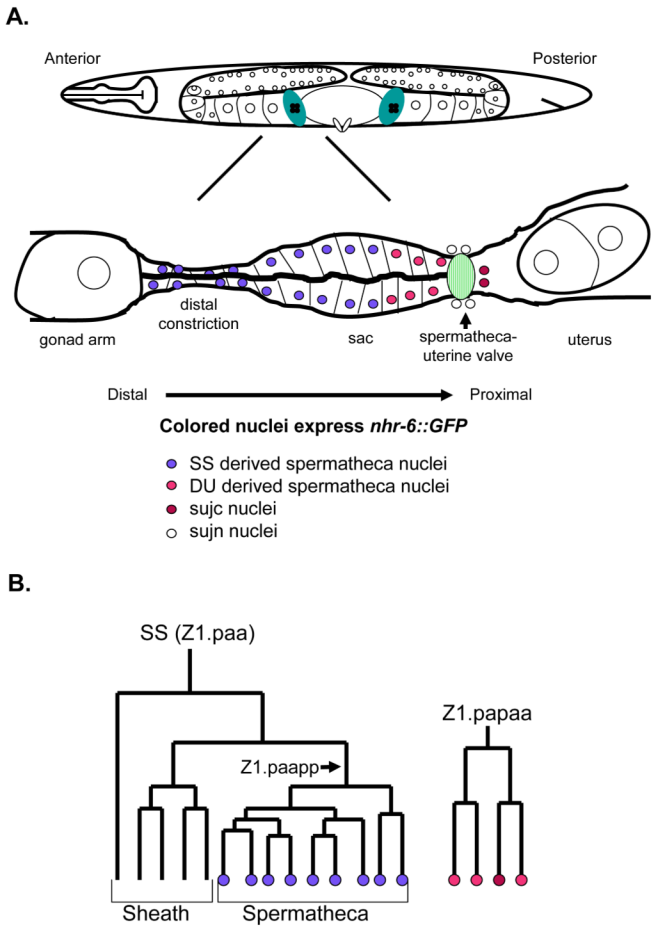

Figure 5. Schematic of the *C. elegans* spermatheca

(A) The anterior spermatheca is shown for an adult hermaphrodite. Distal is left and proximal is right. The spermatheca is shown stretched out for clarity. Normally the spermatheca at this stage is a spiral structure (Kimble and Hirsh, 1979). The positions of nuclei are shown for diagrammatic purposes only and do not reflect the natural positions of spermatheca nuclei in adult hermaphrodites. Sperm are also not indicated for clarity. Colored nuclei express *nhr- 6::GFP.* Different colored nuclei represent different lineages contributing to the spermatheca. (B) One SS cell lineage and one DU lineage that give rise to the anterior spermatheca. Coloration corresponds to the nuclei shown in (A).

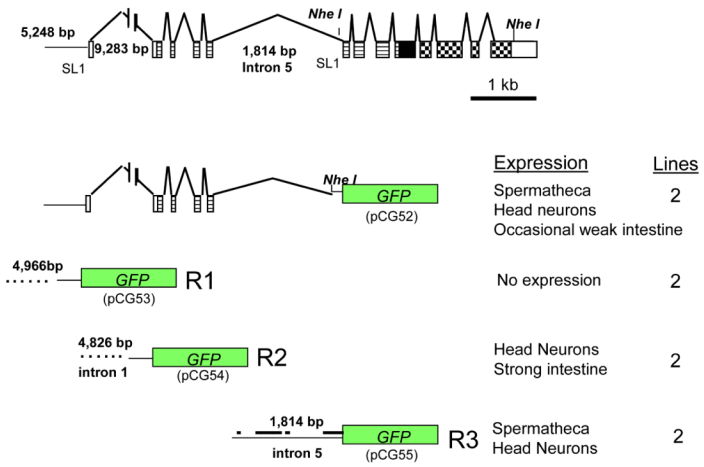

Figure 6. *nhr-6::GFP* reporter constructs

nhr-6::GFP constructs and their correlation to the *nhr-6* gene. pCG52 is considered to incorporate most if not all possible regulatory regions for *nhr-6* as these regions were including in the *nhr-6* genomic rescuing fragment. Transcriptional fusions (pCG53, 54, and 55) of the three potential regulatory regions are shown with their correlation to the full-length reporter. pCG53 contains 4,966 bp of sequence upstream of exon 1. pCG54 contains 4,826 bp of sequence (from intron 1) upstream of exon 2. pCG55 contains all of the sequence from intron 5. Blocks of sequence conservation between intron 5 of *nhr-6* and the identical intron from the *C. briggsae* ortholog of *nhr-6* is indicated by the thick bars in the pCG55 schematic. Only *nhr-6* exon and intron sequences are drawn to scale. Sequences upstream of *GFP* in pCG53 and pCG54 are also not drawn to scale. The sizes in base pairs of these regions are indicated.

NIH-PA Author Manuscript NIH-PA Author Manuscript NIH-PA Author Manuscript

NIH-PA Author Manuscript
NIH-PA Author Manuscript
NIH-PA Author Manuscript

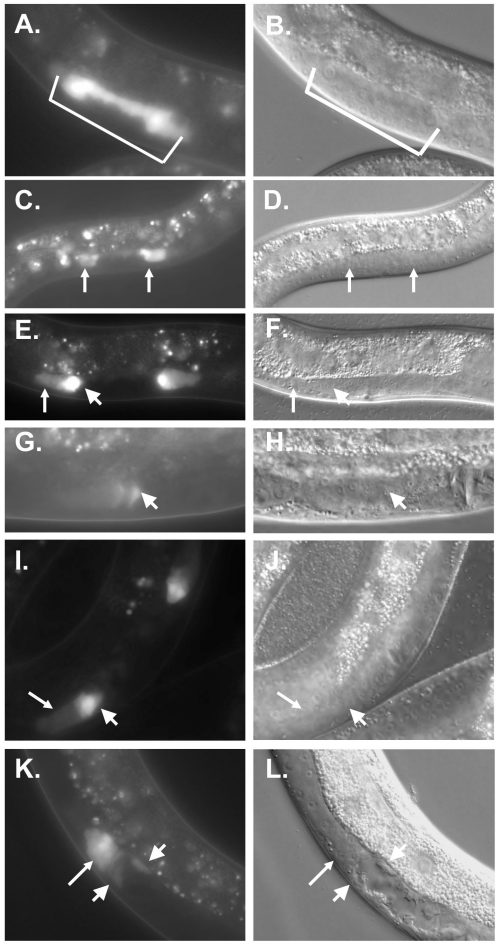

Figure 7. *nhr-6::GFP* expression pattern

Animals in panels (A)-(H) and (K)-(L) bear an integrated full-length *nhr-6::GFP* transgene (*nbIs1000*). Corresponding DIC images are shown on the right for each epifluorescence micrograph. (A, B) Expression in 8 cells (bracket) of a late L3 *nbIs1000* transgenic. (C, D) Expression in early L4 *nbIs1000* transgenic. The arrows indicate the formation of anterior and posterior group of cells expressing the reporter. These cells are presumed to be spermatheca precursors. The animal in this picture is shown at a lower magnification than the other panels. (E, F) Mid-late L4 *nbIs1000* transgenic nematode. Thin arrow indicates expression in the spermatheca and thick arrow indicates higher expression in the sujc cells. (G, H) Young adult *nbIs1000* transgenic nematode. Arrow indicates diminishing expression in the sujc cells. (I, J) L4 nematode transgenic for the *nhr-6R3::GFP* reporter. Arrows indicate spermatheca and sujc cells as in (C). (K, L) Expression of *nhr-6::GFP* in *nhr-6(lg6001)* L4 hermaphrodite. Thin and thick arrows indicate the spermatheca and sujc as above. The sujc in the *nhr-6(lg6001)* mutants do not express brightly and are misplaced within the gonad.

NIH-PA Author Manuscript
NIH-PA Author Manuscript
NIH-PA Author Manuscript

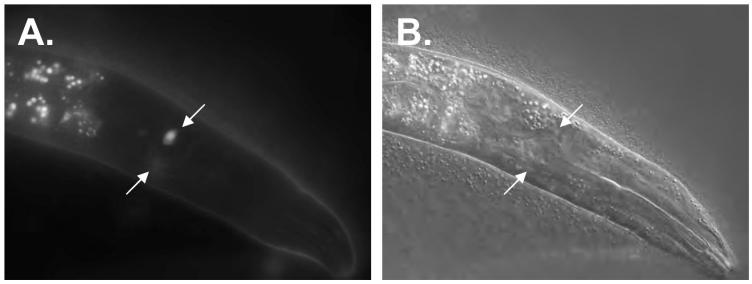

Figure 8. Expression of *nhr-6::GFP* in anterior chemosensory neurons

Epifluorescence (A) and DIC (B) micrographs of an *nbIs1000* trangenic hermaphrodite. Expression in a pair of anterior chemosensory neurons is indicated by the arrows.

NIH-PA Author Manuscript
NIH-PA Author Manuscript
NIH-PA Author Manuscript

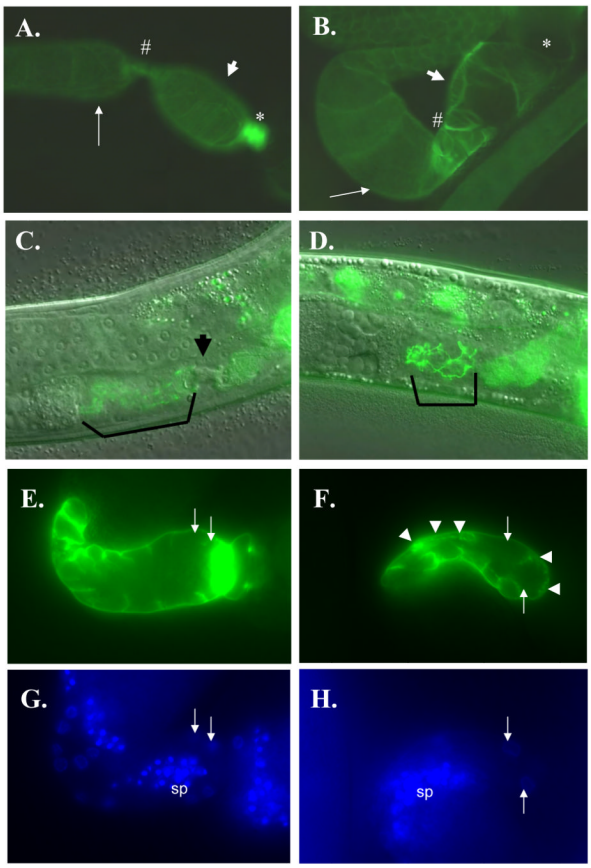

Figure 9. Defective spermatheca differentiation in *nhr-6(lg6001)* mutants

In all micrographs distal is left and proximal is right. FITC-phalloidin of dissected adult gonads (A,B). (A) Dissected gonad from a wild-type adult. Note the circumferentially-oriented actin microfilaments in the spermathecal cells. The proximal oocyte of the gonad arm (thin arrow), the distal spermatheca constriction (#), the spermatheca sac containing a recently ovulated oocyte (thick arrow), and spermatheca-uterine valve (*) are indicated. (B) Dissected gonad from a *nhr-6(lg6001)* adult. Note the abnormal morphology and random pattern of microfilaments of the spermathecal cells. The distal constriction (#) does not have a constricted morphology. The spermatheca sac (thick arrow), also inflated with a recently ovulated oocyte appears to have missing cells, although it is not known if the cells were lost after ovulation or were missing prior to ovulation. Also note the absence of a spermatheca-uterine valve (*). (C, D) AJM-1::GFP expression in a young adult hermaphrodite bearing an integrated *ajm-1::GFP* transgene (*jcIs1*) (merged Nomarski and epifluorescence micrograph) in wild-type (C) and *nhr- 6(lg6001*) mutants (D). The bracket indicates the spermatheca region and the arrow the spermatheca-uterine valve. In both animals AJM-1::GFP illuminates the spermatheca lumen connecting the gonad arm and spermatheca-uterine border. Note decreased size of spermatheca and absence of spermatheca-uterine valve in *nhr-6(lg6001)* mutants. (E-H) MH27 (mouse monoclonal that recognizes AJM-1 protein) immunolocalization (E, F) and corresponding DAPI staining (G, H) of wild-type (E, G) and *nhr-6(lg6001)* (F, H) dissected young adult gonads. Arrows indicate distinct cells by DAPI stained nuclei. Note the cell size and shape differences of the cells in the proximal spermatheca of *nhr- 6(lg6001)*, compared to wild-type. Arrowheads indicate diffuse, mislocalized AJM-1 protein in *nhr-6(lg6001)*. Sp=sperm. In these micrographs, sperm is found in the lumen of the wild-type spermatheca but not the *nhr-6(lg6001)* spermatheca.

NIH-PA Author Manuscript
NIH-PA Author Manuscript
NIH-PA Author Manuscript

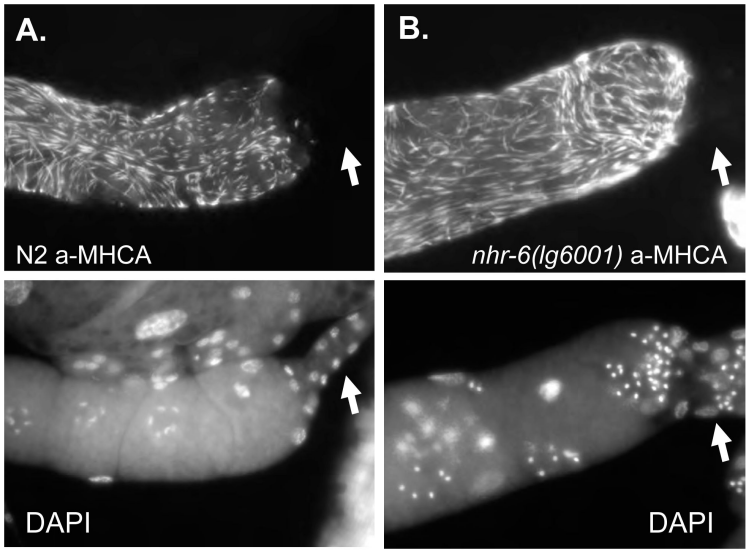

Figure 10. Expression of MHCA in wild-type and *nhr-6(lg6001)* gonads

Epifluorescence micrographs of wild-type (A) and *nhr-6(lg6001)* (B) dissected early adult gonads stained with anti-MHCA (top) and DAPI (bottom). MHCA expression is restricted to the sheath of *nhr-6(lg6001)*, indicating that *nhr-6(lg6001)* spermathecae have not adopted a sheath cell fate. Arrow indicates the spermatheca is present in the dissected gonad preparation. Note the lack of spermathecal distal constriction in the *nhr-6(lg6001)* gonad.

NIH-PA Author Manuscript
NIH-PA Author Manuscript
NIH-PA Author Manuscript

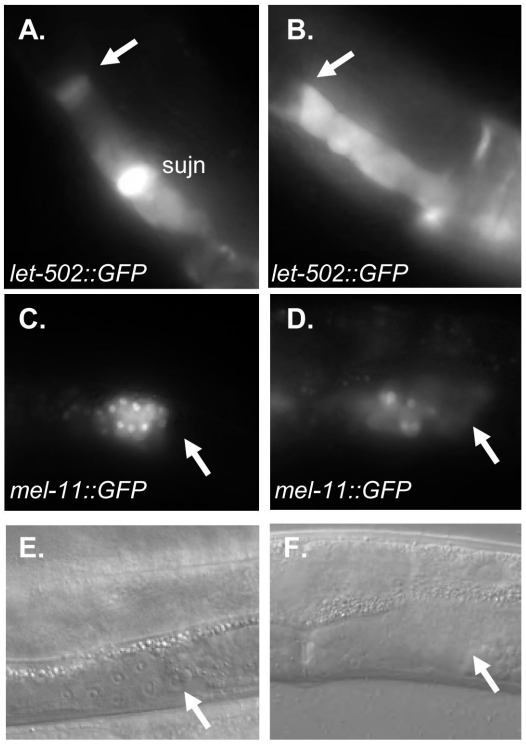

Figure 11. Expression of *let-502::GFP* and *mel-11::GFP* in *nhr-6(lg6001)* hermaphrodites

Expression pattern of *let-502::GFP* (A, B) and *mel-11::GFP* (C, D) in wild-type young adult hermaphrodites (A, C) and *nhr-6(lg6001)* hermaphrodites (B, D). *let-502::GFP* expression is restricted to the proximal and distal regions in wild-type animals while expression is found in all spermathecal cells of *nhr-6(lg6601)* mutants. *mel-11::GFP* is expressed in the spermathecal sac of both wild-type and *nhr-6(lg6001)* mutants. Note the decreased number of expressing nuclei in *nhr-6(lg6001)* mutants. (E, F) DIC micrographs of animals in (C, D). Arrows indicate distal spermatheca. sujn: spermatheca-uterine valve. The spermatheca-uterine valve is not generated in *nhr- 6(lg6001)* mutants.

NIH-PA Author Manuscript
NIH-PA Author Manuscript
NIH-PA Author Manuscript

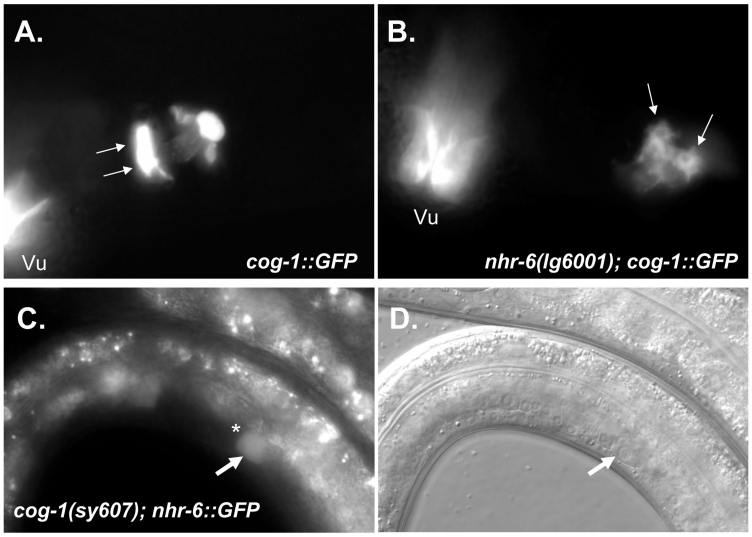

Figure 12. Epistasis analysis *nhr-6::GFP* and *cog-1::GFP*

(A,B) High-magnification epifluorescence micrographs of *cog-1::GFP* (*syIs63)* young adult hermaphrodite (A) and *nhr-6(lg6001); cog-1::GFP* young adult hermaphrodite (B). Arrows indicate the two sujc nuclei. Note in *cog-1::GFP* animals the filopodia that extend from the nuclei in the uterine lumen to the spermatheca. *nhr-6(lg6001); cog-1::GFP* hermaphrodites lack these filopodia and display an abnormal morphology, indicating abnormal differentiation of this structure in *nhr-6(lg6001)* mutants. Vu = *cog-1::GFP* expression in the vulva. (C, D) *nhr-6::GFP (nbIs1000)* expression in L4 *cog-1(sy607)* mutants. The star indicates loss of bright sujc expression (compare to Fig. 7E, F).

NIH-PA Author Manuscript
NIH-PA Author Manuscript
NIH-PA Author Manuscript

Table 1

Reproductive phenotypes in *nhr-6* loss-of-function animals

Genotype	N (adults scored)	Avg. Viable Brood Size	Range
+/+	3	230 ± 32	205-266
nhr-6(lg6001)/nhr-6(lg6001)	35	8 ± 10[1]	0 - 38
nhr-6(lg6001)/nhr-6(tm870)	14	4 ± 7	0- 21
nhr-6(lg6001)/nhr-6(lg6001); nbEx1000	5	182 ± 21	159-205
nhr-6(lg6001)/nhr-6(lg6001); nbEx1010	5	163 ± 45	105-222
nhr-6(lg6001)/qC1 dpy-19(e1259) glp-1(q339)	3	228 ± 34	194-261
eri-1(mg366); nhr-6(RNAi)[2]	8	5 ± 5	2-16
eri-1(mg366); GFP(RNAi)	4	185 ± 24	166-220

[1] Brood size counts include progeny from hermaphrodites that bagged without laying eggs.

[2] It had been previously observed that *nhr-6* RNAi experiments in a wild-type background yield similar phenotypes. However, the phenotypes are less severe and incompletely penetrant (Gissendanner et al., 2004). This indicates that *nhr-6* is somewhat refractory to RNAi in a wild-type background.

NIH-PA Author Manuscript
NIH-PA Author Manuscript
NIH-PA Author Manuscript

Table 2

Abnormal Egg Morphology in *nhr-6* loss-of-function animals

Genotype	N (eggs scored)	% abnormal morphology	% arrest
+/+	99	0	0
nhr-6(lg6001)/nhr-6(lg6001)	152	78	34[1]
nhr-6(lg6001)/nhr-6(lg6001); nbEx1000	66	0	3
nhr-6(lg6001)/nhr-6(lg6001); nbEx1010	93	7.9	0
nhr-6(lg6001)/qC1 dpy-19(e1259) glp-1(q339)	238	0	0
eri-1(mg366); nhr-6(RNAi)	224	59	39[1]
eri-1(mg366); GFP(RNAi)	135	0	0

Eggs scored were collected from 5 adult hermaphrodites (+/+, *nhr-6(lg6001)/nhr-6(lg6001); nbEx1000, nhr-6(lg6001)/nhr-6(lg6001); nbEx1010, nhr-6(lg6001)/qC1, eri-1(mg366); GFP(RNAi)*), 25 adult hermaphrodites (*eri-1(mg366); nhr-6(RNAi)*, or 40 adult hermaphrodites (*nhr-6(lg6001)/nhr-6(lg6001)* during a 24 hour lay period. Embryonic arrest was assessed 24 hours after the end of the lay period.

[1]All arrested eggs displayed abnormal egg morphology.

NIH-PA Author Manuscript
NIH-PA Author Manuscript
NIH-PA Author Manuscript

Table 3

Spermatheca nuclei counts[1]

Experiment	N	# of nuclei	Range
DAPI staining of extruded gonads			
N2	6	24 ± 3	20-27
nhr-6(lg6001)	6	12 ± 1	11-14
nhr-6(+); nhr-6::GFP	21	24 ± 2	20-28
nhr-6(lg6001); nhr-6::GFP	35	10 ± 1	9-12
nhr-6(lg6001); unc-26(e205)ced-3(n717); nhr-6::GFP[2]	10	10 ± 1	8-11
rrf-3(pk1426);fkh-6::GFP	5	24	N/A
rrf-3(pk1426);fkh-6::GFP; nhr-6(RNAi)	10	12 ± 2	10-14

[1]Spermatheca nuclei counts were performed by three methods: DAPI staining of extruded gonads, optical sectioning using *nhr-6::GFP* as a marker, and direct observation of nuclear localized *fkh-6::GFP*. There is some intrinsic error associated with the first two methods that lead to variability in the wild-type spermatheca nuclei counts (all wild-type spermathecae have 24 cells). In addition, the first two methods may sometimes include nuclei from the sujc or sujn. Regardless, nuclei counts for *nhr-6(lg6001)* were consistently decreased compared to wild-type. Unlike *nhr-6::GFP, fkh-6::GFP* is very tightly localized to spermatheca nuclei and is not expressed in the sujc or sujn; therefore, nuclei counts in wild-type background always revealed the normal 24 cell number.

[2]*unc-26(e205)ced-3(n717); nhr-6::GFP* control animals were not directly counted for spermatheca nuclei but microscopic analysis of *unc-26(e205)ced-3(n717)* young adults revealed normal spermatheca size and morphology (data not shown).